

PARAMETRIC ANALYSIS OF INELASTIC INTERACTION IN FRAME-
WALL STRUCTURAL SYSTEMS

A THESIS SUBMITTED TO
THE GRADUATE SCHOOL OF NATURAL AND APPLIED SCIENCES
OF
MIDDLE EAST TECHNICAL UNIVERSITY

BY

SONER SEÇKİNER

IN PARTIAL FULFILLMENT OF THE REQUIREMENTS
FOR
THE DEGREE OF THE MASTER OF SCIENCE
IN
CIVIL ENGINEERING

SEPTEMBER 2011

Approval of the thesis:

PARAMETRIC ANALYSIS OF INELASTIC INTERACTION IN FRAME-WALL STRUCTURAL SYSTEMS

submitted by **SONER SEÇKİNER** in partial fulfillment of the requirements for the degree of **Master of Science in Civil Engineering Department, Middle East Technical University** by,

Prof. Dr. Canan Özgen
Dean, Graduate School of **Natural and Applied Science**

Prof. Dr. Güney Özcebe
Head of Department, **Civil Engineering**

Assoc. Prof. Dr. Afşin Sarıtaş
Supervisor, **Civil Engineering Dept., METU**

Examining Committee Members:

Assoc. Prof. Dr. Erdem Canbay
Civil Engineering Dept., METU

Assoc. Prof. Dr. Afşin Sarıtaş
Civil Engineering Dept., METU

Assoc Prof. Dr. Murat Altuğ Erberik
Civil Engineering Dept., METU

Assist. Prof. Dr. Alp Caner
Civil Engineering Dept., METU

Assist. Prof. Dr. Burcu Güneş
Civil Engineering Dept., Atılım University

Date:

13.09.2011

I hereby declare that all information in this document has been obtained and presented in accordance with academic rules and ethical conduct. I also declare that, as required by these rules and conduct, I have fully cited and referenced all material and results that are not original to this work.

Name, Last name : Soner SEÇKİNER

Signature :

ABSTRACT

PARAMETRIC ANALYSIS OF INELASTIC INTERACTION IN FRAME-WALL STRUCTURAL SYSTEMS

Seçkiner, Soner

M.Sc., Department of Civil Engineering

Supervisor: Assoc. Prof. Dr. Afşin Sarıtaş

September 2011, 74 pages

The purpose of this thesis is to investigate the inelastic action in the reinforced concrete frame-wall structures analytically and with that analysis to follow the plastic formation of the structure. For this purpose, six mid-rise reinforced concrete buildings with frame-wall are modeled and analyzed to understand the effect of the height and base shear force ratio of the wall on the nonlinear interaction between reinforced concrete wall and frame members under static lateral loads and ground motion excitations. The parametric analysis is conducted by assuming planar response of the buildings under loadings.

The buildings are generated considering the limit design concept suggested by Turkish Earthquake Code 2007 and Turkish Standards TS500, and the frame-wall members are modeled by using spread plasticity elements and fiber discretization of sections. In the analysis stage, each element section is divided into confined and unconfined regions for detailed modeling of the building by using OpenSEES nonlinear finite element program. Two dimensional analyses are conducted under static and dynamic loadings. For static pushover analyses, three different lateral load cases (Triangular, Uniform and First-Mode Lateral Load Patterns) are

considered. For dynamic analyses, eight different ground motions are used. These ground motions are scaled to the corresponding design response spectrum suggested by Turkish Earthquake Code 2007 by using RSPMATCH program. Using the result of the complex and simplified analyses, inter-story drift ratios, plastic rotations and internal force distributions of the buildings are investigated.

Keywords: Frame-wall structures, reinforced concrete shear wall, nonlinear analysis, frame-wall interaction

ÖZ

DUVAR-ÇERÇEVE YAPISAL SİSTEMLERDE ELASTİK OLMAYAN ETKİLEŞİMİN PARAMETRİK ÇÖZÜMLENMESİ

Seçkiner, Soner

Yüksek Lisans, İnşaat Mühendisliği Bölümü

Tez Yöneticisi: Doç. Dr. Afşin Sarıtaş

Eylül 2011, 74 sayfa

Bu tezin amacı çerçevesi ve duvarlı betonarme yapıların doğrusal olmayan davranışını analitik olarak incelemek ve bu analizlerle binada meydana gelen plastikleşmeyi takip etmektir. Bu amaca yönelik olarak altı adet orta yükseklikte çerçevesi ve duvarlı betonarme binanın tasarımı yapılmıştır. Bu binaların tasarımındaki parametrik farklılıklar toplam bina yüksekliği ve duvar tabanında taşınan kesme kuvveti oranı sonucudur. Binaların tepkisinin düzlemsel kaldığı varsayılmış ve statik ve dinamik yüklemeler altında analizleri yapılarak çerçeve ve duvar elemanları arasındaki doğrusal olmayan etkileşim incelenmiştir.

Çalışmada dikkate alınan binalar Türk Deprem Yönetmeliği 2007'deki ve Türk Standartları TS500'deki limit dizayn önerileri gözetilerek tasarlanmıştır. Çerçeve-duvar sistemin tüm elemanları yayılı plastisite elemanları ve fiber kesit modelleri kullanılarak modellenmiştir. Doğrusal olmayan analiz OpenSEES sonlu elemanlar programı kullanılarak gerçekleştirilmiştir. Her bir kolon, giriş ve duvar kesidi üstünde sargılı ve sargısız betonarme bölgelerin davranışı dikkate alınmış ve doğrusal olmayan malzeme modelleri kullanılmıştır. Binaların analizi aşamasında davranışın düzlemsel olduğu varsayılarak statik ve dinamik analizler yapılmıştır. Statik öteleme analizi için üç farklı yatay yükleme (Üçgen, Düzgün Yayılı ve İlk-

mod Yatay Yükleme Şablonları) kullanılmıştır. Dinamik analizler için, sekiz farklı yer hareketi kullanılmıştır. Bu yer hareketleri, Türk Deprem Yönetmeliği 2007’de tavsiye edilen ivme spektrumuna RSPMATCH programı kullanılarak ölçeklenmiştir. Bu kompleks ve basitleştirilmiş analizlerin kullanılması sonucunda, katlar arası ötelenmeler, kritik elemanlarda meydana gelen plastik dönmeler ve içsel yük dağılımları incelenmiştir.

Anahtar Kelimeler: Çerçeve-duvar binalar, betonarme duvar, doğrusal olmayan analiz, çerçeve-duvar etkileşimi

To My Family

ACKNOWLEDGEMENTS

The author would like to express his sincere appreciation to his supervisor Assoc. Prof. Dr. Afşin Sarıtaş for his supervision, guidance, encouragement and patience throughout this study.

The scholarship provided by the Scientific and Technological Research Council of Turkey (TÜBİTAK) is gratefully acknowledged.

I would like to thank Assoc. Prof. Dr. Erdem Canbay and Assoc. Prof. Dr. Sinan Akkar for their comments and suggestions throughout this study.

TABLE OF CONTENTS

ABSTRACT	iv
ÖZ.....	vi
ACKNOWLEDGEMENTS.....	ix
TABLE OF CONTENTS	x
LIST OF TABLES.....	xii
LIST OF FIGURES	xiii
CHAPTERS	
1. INTRODUCTION.....	1
1.1 GENERAL.....	1
1.2 RESEARCH OBJECTIVE AND SCOPE	3
2. LITERATURE SURVEY	5
2.1 INTRODUCTION	5
2.3 NONLINEAR INTERACTION IN FRAME-WALL.....	5
3. MODELLING AND ANALYSING FRAME ELEMENTS.....	11
3.1 INTRODUCTION	11
3.2 BUILDING MODEL	11
3.3 ELEMENT MODEL.....	18
3.3.1 Beam Element	18
3.3.2 Column and Shear Wall Elements.....	21
3.4 MATERIAL PROPERTIES	24

3.5	OpenSEES.....	26
3.6	SCALING AND SELECTION OF GROUND MOTIONS	28
3.7	RSPMATCH	31
4.	RESULTS AND DISCUSSION	32
4.1	INTRODUCTION	32
4.2	STATIC PUSHOVER ANALYSES.....	33
4.2.1	Pushover Results of Selected Elements.....	36
4.2.2	Plastic Rotation of Selected Elements	41
4.2.3	Inter-Story Drift.....	45
4.2.4	Patterns of Static Load Effects	47
4.2.5	Comparison of Wall Base Shear Ratio.....	51
4.3	NONLINEAR DYNAMIC ANALYSES	54
4.3.1	Time-History Analyses Results.....	55
4.3.2	Plastic Rotation of Selected Elements.....	60
4.3.3	Patterns of Shear Force Distributions.....	63
4.4	SUMMARY	67
5.	CONCLUSION	69
5.1	CONCLUSION.....	69
5.2	RECOMMENDATIONS FOR FUTURE RESEARCH.....	71
	REFERENCES	72

LIST OF TABLES

TABLES

Table 3.1 The Properties of Selected Buildings	13
Table 3.2 Elastic Base Shear Force Ratio of Wall.....	17
Table 3.3 Member Size of Selected Buildings	18
Table 3.4 Properties of Employed Ground Motions.....	29
Table 4.1 Comparison of Inelastic Base Shear Force Ratio of Wall at 0.0% Roof Drift Ratio	52
Table 4.2 Comparison of Inelastic Base Shear Force Ratio of Wall at 0.5% Roof Drift Ratio	53
Table 4.3 Comparison of Inelastic Base Shear Force Ratio of Wall at 2.0% Roof Drift Ratio	54

LIST OF FIGURES

FIGURES

Figure 2.1 Deformation Modes of Frame-Wall Structures (Emori and Schnobrich, 1978).....	7
Figure 2.2 Typical Deflection of Frames (Goodsir et al., 1982)	8
Figure 2.3 Lumped Frames of Building (Goodsir et al., 1982).....	9
Figure 2.4 Plan View of Building (Goodsir et al., 1982)	9
Figure 3.1 Lumped View of Selected Frames	14
Figure 3.2 Plan View of F1, F2, F3	15
Figure 3.3 Plan View of F4, F5, F6	16
Figure 3.4 Sectional Dimension of Beams	20
Figure 3.5 Dimensions of Columns	21
Figure 3.6 Regions in Shear Wall.....	22
Figure 3.7 Details of Shear Wall	23
Figure 3.8 Concrete01 Material Model (Mazzoni et al., 2007).....	25
Figure 3.9 Steel02 Material Model (Mazzoni et al., 2007)	26
Figure 3.10 Fiber Discretization of Beam-Column Element (Taucer et al., 1991).....	27
Figure 3.11 Spectral Acceleration vs. Period for Unscaled Ground Motions (5% Damped)	30
Figure 3.12 Spectral Acceleration vs. Period for Scaled Ground Motions (5% Damped)	30
Figure 4.1 Applied Static Lateral Load Patterns	33

Figure 4.2 Total Base Shear vs. Roof Drift Ratio – Triangular Pushover Analysis	34
Figure 4.3 Total Base Shear vs. Roof Drift Ratio – Uniform Pushover Analysis..	34
Figure 4.4 Total Base Shear vs. Roof Drift Ratio – First-Mode Pushover Analysis	35
Figure 4.5 Wall Base Shear vs. Roof Drift Ratio – Triangular Pushover Analysis	36
Figure 4.6 Wall Base Shear vs. Roof Drift Ratio – Uniform Pushover Analysis..	37
Figure 4.7 Wall Base Shear vs. Roof Drift Ratio – First-Mode Pushover Analysis	37
Figure 4.8 Total Column Base Shear vs. Roof Drift Ratio – Triangular Pushover Analysis	39
Figure 4.9 Total Column Base Shear vs. Roof Drift Ratio – Uniform Pushover Analysis	39
Figure 4.10 Total Column Base Shear vs. Roof Drift Ratio – First-Mode Pushover Analysis	40
Figure 4.11 Story vs. Maximum Plastic Rotation for Middle Column – Pushover Analysis	42
Figure 4.12 Story vs. Maximum Plastic Rotation for Wall – Pushover Analysis .	44
Figure 4.13 Story vs. Inter-Story Drift Ratio – Triangular Pushover Analysis.....	45
Figure 4.14 Story vs. Inter-Story Drift Ratio – Uniform Pushover Analysis	46
Figure 4.15 Story vs. Inter-Story Drift Ratio – First-Mode Pushover Analysis....	46
Figure 4.16 The Total Internal Force Distributions in Columns at the end of Triangular Pushover Analysis.....	48

Figure 4.17 The Total Internal Force Distributions in Columns at the end of Uniform Pushover Analysis.....	48
Figure 4.18 The Total Internal Force Distributions in Columns at the end of First-Mode Pushover Analysis	49
Figure 4.19 The Total Internal Force Distributions in Wall at the end of Triangular Pushover Analysis	50
Figure 4.20 The Total Internal Force Distributions in Wall at the end of Uniform Pushover Analysis	50
Figure 4.21 The Total Internal Force Distributions in Wall at the end of First-Mode Pushover Analysis	51
Figure 4.22 Normalized Base Shear vs. Maximum Roof Drift for All Buildings – Time-History Analysis.....	55
Figure 4.23 Story vs. Max. Inter-Story Drift Ratio for All Buildings – Time-History Analysis of Gm1	56
Figure 4.24 Story vs. Max. Inter-Story Drift Ratio for All Buildings – Time-History Analysis of Gm2	56
Figure 4.25 Story vs. Max. Inter-Story Drift Ratio for All Buildings – Time-History Analysis of Gm3	57
Figure 4.26 Story vs. Max. Inter-Story Drift Ratio for All Buildings – Time-History Analysis of Gm4	57
Figure 4.27 Story vs. Max. Inter-Story Drift Ratio for All Buildings – Time-History Analysis of Gm5	58
Figure 4.28 Story vs. Max. Inter-Story Drift Ratio for All Buildings – Time-History Analysis of Gm6	58

Figure 4.29 Story vs. Max. Inter-Story Drift Ratio for All Buildings – Time- History Analysis of Gm7	59
Figure 4.30 Story vs. Max. Inter-Story Drift Ratio for All Buildings – Time- History Analysis of Gm8	59
Figure 4.31 Plastic Rotation of Middle Column – Time-History Analysis	61
Figure 4.32 Plastic Rotation of Wall – Time-History Analysis.....	62
Figure 4.33 Story vs. Maximum Total Shear Force / Total Base Shear for Columns – Time-History Analysis	64
Figure 4.34 Story vs. Maximum Shear Force / Total Base Shear for Wall – Time- History Analysis	65

CHAPTER 1

INTRODUCTION

1.1 GENERAL

Structural walls or more popularly called as shear walls provide significant lateral rigidity to moment resisting frame systems; thereby reducing displacement demands on structural components that are either primary or secondary to the building. In recent years, the need to use shear walls has furthermore increased especially in earthquake prone regions. Researchers observed that a well-designed shear-wall when introduced in a moment resisting frame provides increased energy dissipation during severe earthquakes.

Shear walls in high seismic regions should be well designed because prior observations showed that the buildings did not reveal good performance even if they have high wall area to floor area. It is also known that the moment resisting frame system is sometimes insufficient to carry lateral loads during severe earthquakes.

According to Turkish Earthquake Code (TEC), frame-wall systems can be classified in two groups;

- High ductile frame-wall system which is composed of high ductile frame and high ductile shear wall,

- Mixed type frame-wall system which is composed of normal ductile frame and high ductile shear wall.

Reinforced concrete walls are regarded as effective lateral force resisting members and they are capable of conferring good performance to structures subjected to wind and earthquake. Their resistance against earthquake forces provides enough strength to the building that it can survive under strong ground motion with only limited structural damage. As a result, the nonstructural components are not damaged during earthquake strike, as well (Tjhin, Aschheim, Wallace, 2006).

While designing buildings, the important point is to decide the sufficient lateral resistance against earthquakes, winds and blast loads. These forces can produce high stresses and induce vibrations. Reinforced concrete walls are often chosen because they provide reliable and economical solution to resist such lateral forces. Columns have also contribution to the lateral resistance but their contribution is much smaller than reinforced walls (Schnobrich, 1977).

Practical engineers use elastic analysis methods for the design of the buildings because it is easy to implement and TEC allows them to use elastic analysis. However, recent observations show that the response of frame-wall systems is often in the inelastic range when a strong lateral force due to earthquake force is acting on the building. Moreover, nowadays contemporary researchers and engineers frequently use inelastic analysis to understand the behavior of buildings. The nonlinear approach is much more realistic than elastic approach. Therefore, the inelastic analysis approach should be preferred while designing and analyzing the response of buildings, especially if they have complex force redistribution mechanisms between various load carrying components. Generally, two types of nonlinear behavior is studied; material nonlinearity and geometric nonlinearity.

Combination of material and geometric nonlinearities results in complex nonlinear stress variations in the members when compared with the stress variations obtained by first-order linear elastic analysis. This stress variation is very important to identify the failure mechanism observed in frame-wall system. Therefore, the frame-wall systems must be studied by considering the nonlinear behavior of components (Kayal, 1986).

It can be concluded that shear-wall has an important role in nonlinear lateral load analysis of the building systems. Because of this reason, the nonlinear interaction between frame-wall should be investigated carefully in the building system.

1.2 RESEARCH OBJECTIVE AND SCOPE

The purpose of this thesis is to investigate analytically the inelastic behavior of the reinforced concrete planar frame-wall structures and with that analysis to follow the force redistribution process and the overall plastic formation of the structure.

Six mid-rise reinforced concrete buildings with frame-wall system are designed according to the TEC (Turkish Earthquake Code 2007) and Turkish Standards TS500. The buildings are analyzed and modeled to understand the influence of the height of building and the base shear force ratio of wall on the nonlinear interaction between reinforced concrete wall and frame members under static lateral loads and ground motion excitation.

This thesis is composed of five chapters. In Chapter 2, brief information about past researches about nonlinear analyses on frame-wall buildings will be presented. In Chapter 3, modeling details of the building will be introduced and the analyses details will be given. In Chapter 4, results of the nonlinear seismic

and static analyses results will be compared with the different analyses cases. Finally, the conclusion will be presented in Chapter 5.

CHAPTER 2

LITERATURE SURVEY

2.1 INTRODUCTION

The inelastic force redistribution in frame-wall buildings should be investigated first in order to prevent collapse of the structure (Emori, Schnobrich, 1978). In this regard, choosing an accurate and relatively simple finite element model suitable for the nonlinear analysis of the reinforced concrete frame-wall buildings is very important. Many researches have been reported about nonlinear behavior of reinforced concrete frame-wall buildings and finite elements methods. In this chapter, past researches about inelastic interaction in frame-wall structures and finite element models are discussed.

2.3 NONLINEAR INTERACTION IN FRAME-WALL

Clark (1968)

This is one of the earliest research study published on the nonlinear behavior of frame-wall structures. The aim of the study was to predict the behavior of large planar reinforced concrete frame-wall structures through the consideration of material and geometric nonlinearity in analysis. In the analysis, the nonlinear material behavior was introduced at the member level through the use of elastic perfectly plastic moment-curvature relationships. A computer program was developed using Fortran programming language. The equations of equilibrium were solved by an iterative procedure. Two 20-storey and 2-bays reinforced

concrete buildings were analyzed to understand the nonlinear behavior of frame-wall systems. This study showed that differences in the stress levels in the columns and shear wall can produce early hinging in the girders. Moreover, examination of slenderness effects suggests that instability over several storeys can arise if the structure is sufficiently slender. Increasing of the shear wall stiffness cannot affect the failure load significantly (Clark, 1968).

Takayagani and Schnobrich (1976)

Takayagani and Schnobrich (Takayagani, Schnobrich, 1976) modeled a 10-storey building with a multiple spring beam model. For the inelastic analyses of the reinforced concrete wall, they divided the wall element into subelements. Each subelement has a uniform flexural rigidity that changes based on the hysteresis loop appropriate to each subelement. Moreover, the layering concept was utilized to analyze the inelastic behavior of reinforced concrete wall members. Each layer had material behavior characteristics that depended on the stress-strain curve of its material in its current deformation. At the end of the analyses, they observed that inelastic action of the connecting beams to the wall started earlier and inelastic action started in intermediate story levels and it spread to the upper and lower story level of the building during static analyses. During the time-history analyses, mode shapes of the structure did not change significantly and substantial reduction of stiffness was observed.

Emori and Schnobrich (1978)

These researchers investigated the nonlinear response of frame-wall systems through both experimental and analytical studies. In their numerical study, geometric nonlinear response was not taken into account, and three different types of models were used to simulate the nonlinear material response of components; namely a concentrated spring model, a multiple spring model, and a layered model. Two 10-storey 3-bays buildings (See Figure 2.1) were selected. Strong column weak beam concept was used in design phase. Dynamic analyses were

conducted, and the results were compared with experimental results. The research demonstrated remarkable results that inelastic actions play a major role in controlling the structural response of frame-wall type structures. The results obtained through the use of multiple spring models demonstrated detailed inelastic behavior in shear-walls. Frequencies of the structure decrease considerably during the earthquake motion reflecting a significant reduction of structural component rigidities.

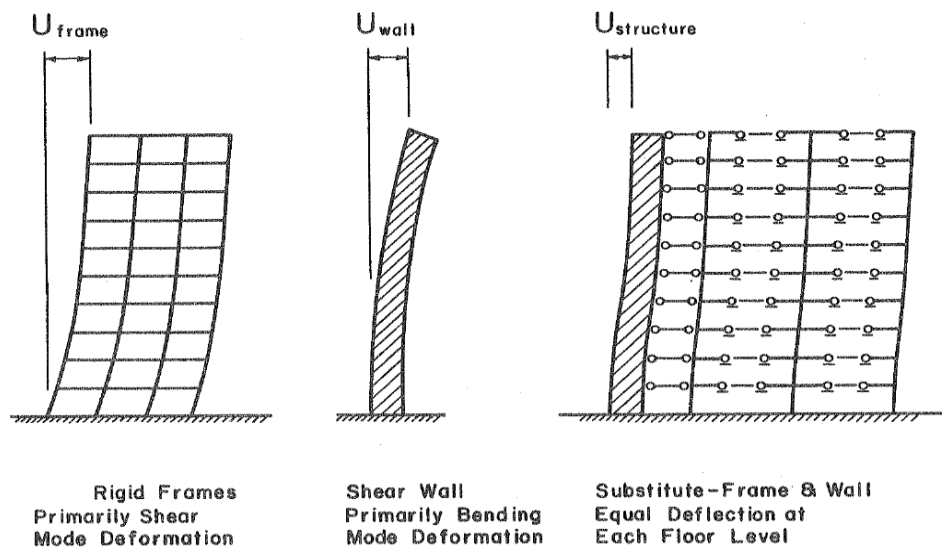


Figure 2.1 Deformation Modes of Frame-Wall Structures (Emori and Schnobrich, 1978)

Goodsir et al. (1982)

Goodsir et al. (Goodsir, Paulay, Carr, 1982) studied inelastic response of three 12-storey buildings (See Figure 2.2). The structures composed of seven 2-bays frames, eight 1-bay frames and a range of three pairs of shear walls which provided variation in stiffness distribution. Design of the buildings was conducted by application of capacity design principles to the result of preliminary elastic analyses. Nonlinear dynamic analysis was conducted, and El Centro N-S, 1940 and Pacoima Dam S14°W, 1971 excitations were used.

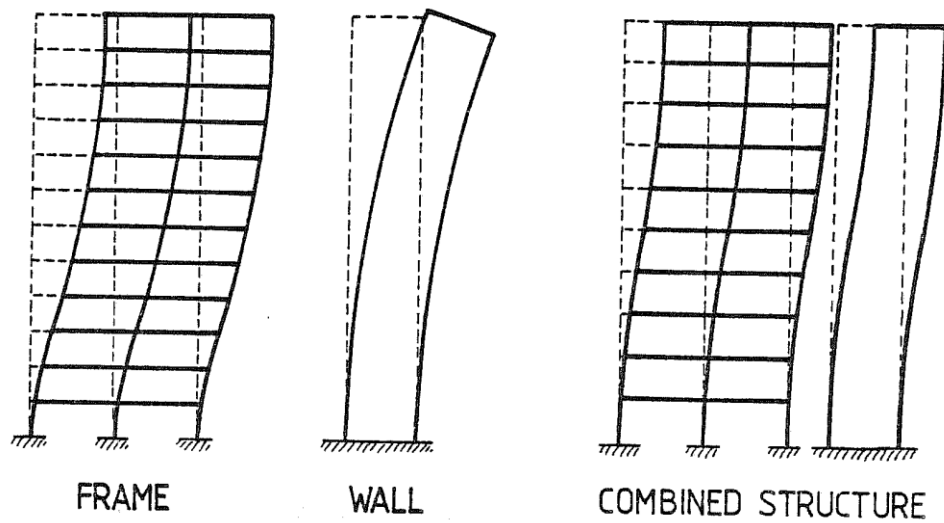


Figure 2.2 Typical Deflection of Frames (Goodsir et al., 1982)

In order to reduce required time and capacity for the analysis of the structural system, Goodsir et al. used the lumped frames and lumped walls as shown in Figures 2.3 and 2.4. They stated that simplifying the structural model by lumping the frames and walls provided a convenient approach for a parametric analysis where the response of the building was assumed to remain in the plane. To investigate the report deeper, Goodsir et al. compared cracked and uncracked frame and wall elements with inelastic material models by conducting static lateral load analyses and dynamic analyses. At the end of the analyses, Goodsir et al. concluded that the buildings showed good resistance to the seismic attack. In addition, they observed that the structures show similar deflections and maximum displacement, and as the wall size increased, the fluctuations on the displacement decreased.

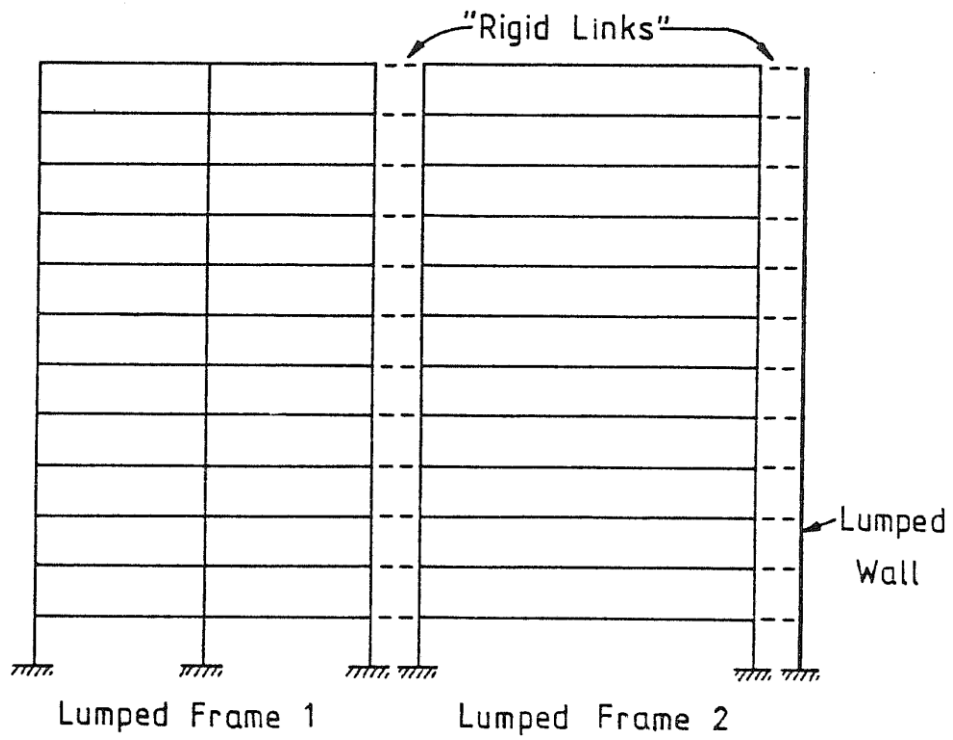


Figure 2.3 Lumped Frames of Building (Goodsir et al., 1982)

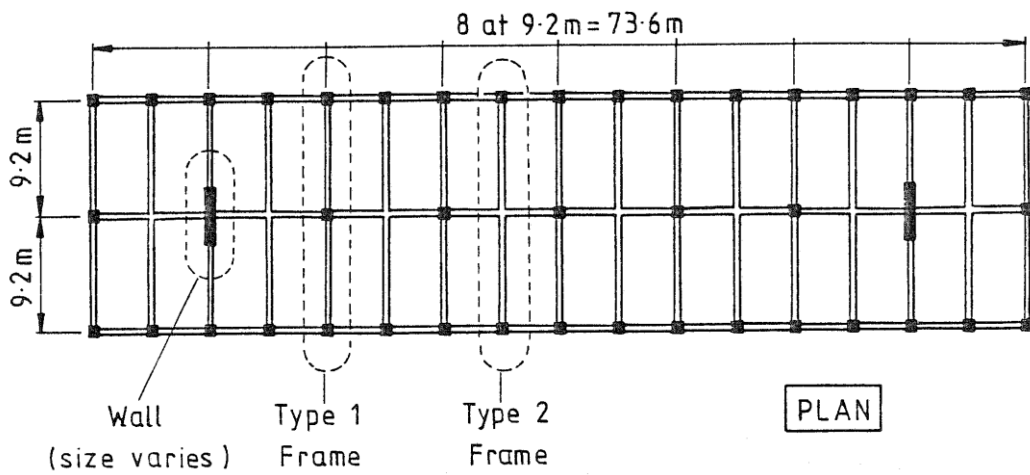


Figure 2.4 Plan View of Building (Goodsir et al., 1982)

Park, Reinhorn, Kunnath (1987)

Park et al. (Park, Reinhorn, Kunnath, 1987) developed an inelastic analysis program. This program is called IDARC (Inelastic Damage Analysis of Reinforced Concrete Frame-Shear Wall Structures). IDARC has become popular since 1987 and various version of the program has been developed by Park et al (1987). Park et al. used a 7-story building, and modeled the shear-wall and frame elements by using fiber sections and inelastic material and nonlinear geometry properties. They modeled the shear-wall with the fiber section column element and they used rigid end zones for the wall element. They concluded that the experimental results and analytical computations matched.

Akış (2004)

Akış studied the three dimensional behavior of frame-wall structures with the purpose of finding the optimum shear wall orientation under dynamic and static analysis. The analyses were performed by using Sap2000 and Etabs programs assuming the buildings remain in the elastic range. Akış stated that wide column analogy for shear walls can be used for the analysis of multistory buildings where rigid diaphragm floor is valid.

Amiri et al. (2008)

Amiri et al. (Amiri, Ahmadi, Ganjavi, 2008) investigated the inelastic behavior of frame-wall structures under dynamic analysis. They selected 8-, 12-, 15-storey buildings for their study and compared the responses of the buildings in terms of the drift distribution, hysteric energy, and damage index and top-story displacement under ten severe earthquakes by using IDARC 2D finite element program. They observed that the damage in the columns was negligible in each story because of the strong-column and weak-beam consideration. And roof floor experienced less damage than other story levels.

CHAPTER 3

MODELLING AND ANALYSING FRAME ELEMENTS

3.1 INTRODUCTION

This chapter gives information about the analysis methods and selected structural systems considered in the thesis. Furthermore, the analysis approach and analytical models used for the components are discussed. For detailed comparison of the inelastic interaction between the wall and the frame, six reinforced concrete frames and eight ground motions are employed.

Two mid-rise frame sets used in this study contain 10- to 15-storey frames including various numbers of bays. Identified according to the names F1, F2, F3 for 10-storey buildings and F4, F5, F6 for 15-storey buildings, the buildings have 2-bay to 12-bay frames.

The ground motion records are selected from Strong Motion Database, Pacific Earthquake Engineering Research Center (PEER) in order to compare and contrast the inelastic behavior between wall and frame better.

3.2 BUILDING MODEL

The structural models are generated considering the limit design concept suggested by TEC (Turkish Earthquake Code, 2007) and Turkish Standards TS500 (2000). The shear force ratio of the wall to frame is changing in the range

of 0.40 to 0.75 which are limit values for high ductile buildings and mixed type of buildings in TEC. It is worth to mention that these ratios are values obtained from elastic analyses calculated by using gross moment of inertia of structural components.

In Chapter 2, it was mentioned that Goodsir et al. analyzed frame systems composed of variable frame and wall systems. Goodsir et al. lumped the frame systems and wall systems into the plane for easy parametric analysis (Goodsir, Paulay, Carr, 1982). The study presented in this thesis also takes advantage of the convenience of planar analysis by lumping frames as suggested by Goodsir.

Six building models are studied in this thesis. The elastic analyses as part of the design phase are conducted using the ETABS finite element program (Wilson, Dovey, Habibullah, 1997), and by following the guidelines presented in TEC and TS500. Buildings are designed as high ductile frame wall systems. Probina (2010) is used to check the design of the buildings. Strong column and weak beam design concept is followed.

In the building models, C30 concrete and S420 steel is used. The height of the building is 30 m. for F1, F2, F3 frames and 45 m. for F4, F5 and F6 frames. Number of story is 10 and 15 as shown in Table 3.1. Total mass of buildings are changing between 753.1 tons and 5261.4 tons and fundamental period of the buildings are changing from 0.68 sec. to 1.92 sec. as shown in Table 3.1.

Table 3.1 The Properties of Selected Buildings

FRAME	Total Mass (tons)	Story #	Fundamental Period T1 (sec)	Story Height (m)	Number of Frame Bays	Number of Wall Bays
F1	753.1	10	1.12	3	2	1
F2	2030.4	10	0.82	3	6	1
F3	3309.02	10	0.68	3	10	1
F4	2140.65	15	1.92	3	2	3
F5	3388.95	15	1.77	3	6	3
F6	5261.4	15	1.42	3	12	3

Slab thickness of the buildings is 12 cm and building is composed of either 5 m or 3.5 m beams. All of the slabs are 5 m x 5 m in dimension. Two dimensional view of building is presented in Figure 3.1, where wall and frames are lumped at the right of the rigid link and frames are lumped at the left of the building. Once again, F1, F2 and F3 have ten stories and F4, F5, F6 have fifteen stories.

In Figure 3.2, the plan view of F1 to F3 buildings are shown. F1 has two bays of frames and one bay of wall, F2 has six bays of frames and one bay of wall and F3 has ten bays of frames. In Figure 3.3, plan view of F4 to F6 buildings are shown. F4 has two bays of frames and three bays of wall, F5 has six bays of frames and three bays of wall and F6 has twelve bays of frames and three bays of wall.

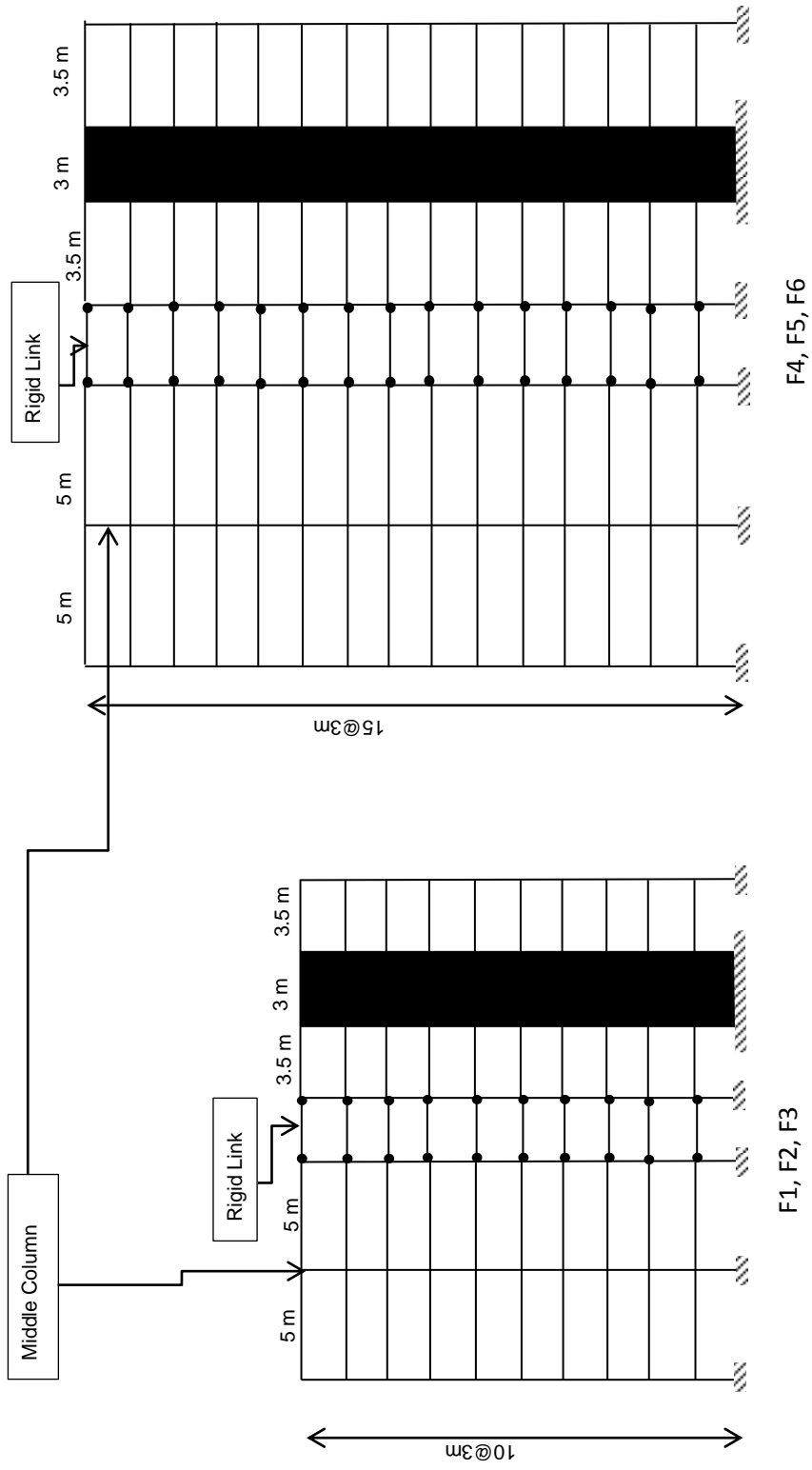


Figure 3.1 Lumped View of Selected Frames

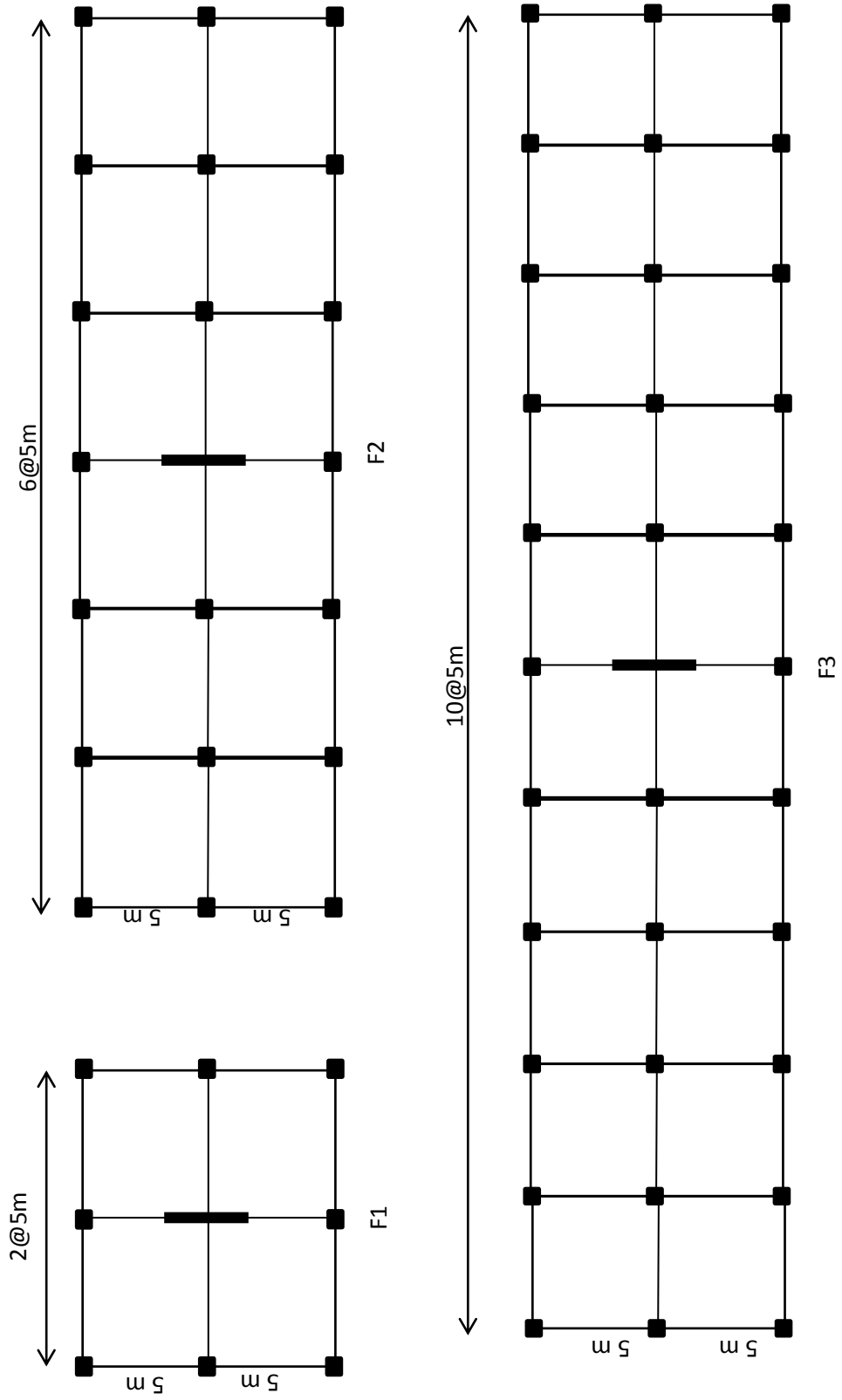


Figure 3.2 Plan View of F1, F2, F3

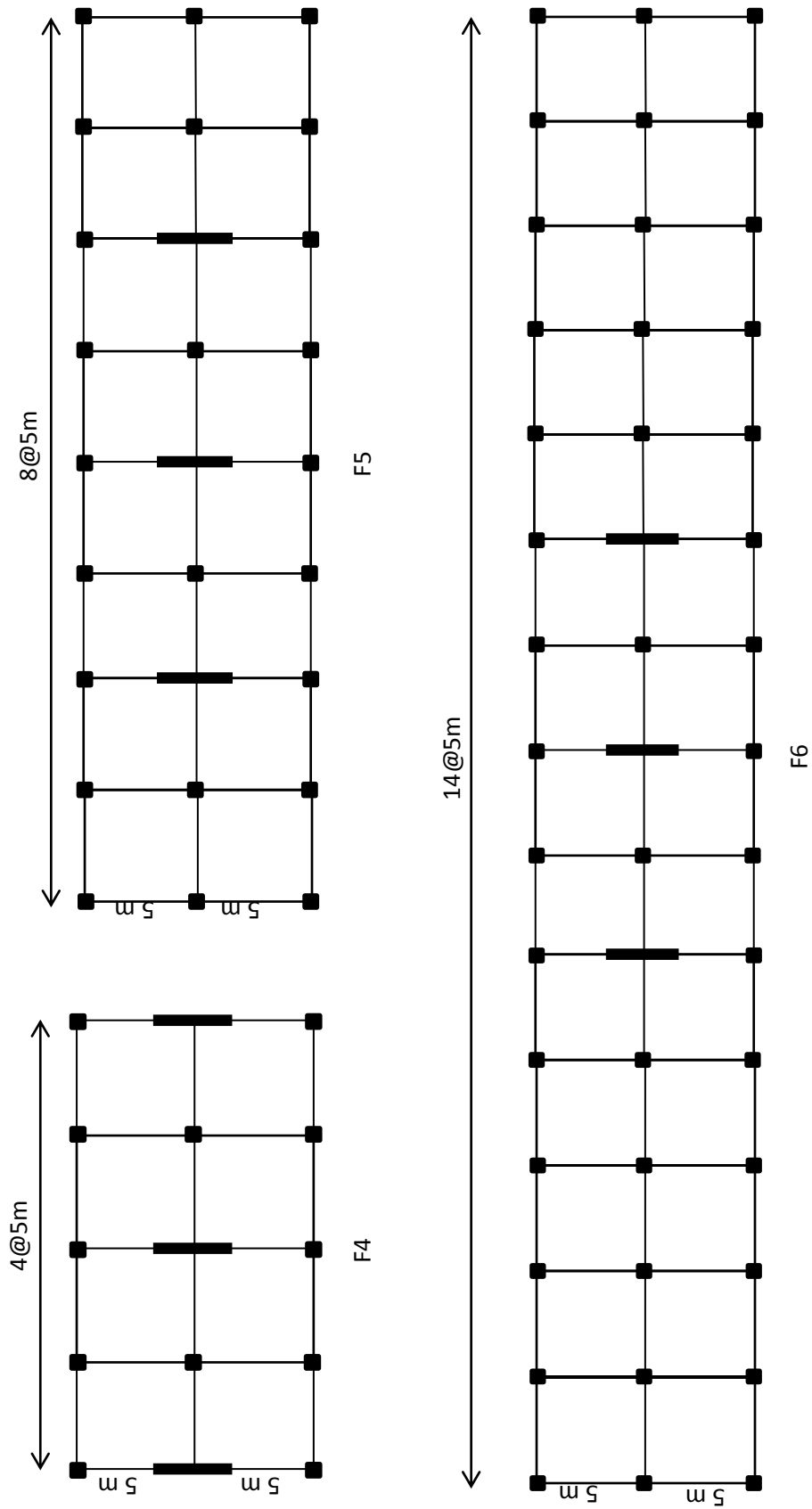


Figure 3.3 Plan View of F4, F5, F6

The static analyses are performed by using ETABS program and the designs are controlled and verified by Probina. It is assumed that the buildings are in Zone 1 according to TEC and the buildings are residential buildings. All of the members are assumed to be highly ductile. Only the flexural design is conducted, and it is assumed that buildings are resistant to shear forces and shear design is not considered. Strong column weak beam design is strictly checked at each beam-column connection. Nonlinear analyses are performed in Open System for Earthquake Engineering Simulation (OpenSEES) by using nonlinear material models specified at stress-strain level over a cross-section of every member in the buildings (Mazzoni, McKenna, Scott, Fenves, 2009). It was assumed that the nonlinear response was mainly affected by material behavior.

Table 3.2 Elastic Base Shear Force Ratio of Wall

FRAME	Elastic Base Shear Force Ratio of Wall %
F1	75.2
F2	57.1
F3	46.5
F4	73.1
F5	57.7
F6	44.2

Table 3.2 shows the ratio of elastic base shear force of wall to the total base shear force in the selected buildings designed for the parametric analyses. The values in the table are obtained from the analysis of the buildings in ETABS by using gross moment of inertia for the calculation of flexural rigidity of structural components as suggested by TEC and TS 500. The shear force ratio is changing from 0.40 to 0.75, falling in the range suggested by TEC.

3.3 ELEMENT MODEL

The member size of different buildings is shown in Table 3.3. The dimensions are confirming to the guidelines in TEC 2007 and TS500. The columns are selected as 0.5 m x 0.5 m for F1 to F3 buildings and 0.7 m x 0.7 m for F4 to F6 buildings. The beams are selected as 0.25 m x 0.55 m for all buildings. In Table 3.3, the dimension of members is constant over the height of the building.

Table 3.3 Member Size of Selected Buildings

FRAME	Wall Dimension (m)	Column Dimension (m)	Beam Dimension (m)
F1	3 x 0.25	0.5 x 0.5	0.25 x 0.55
F2	3 x 0.25	0.5 x 0.5	0.25 x 0.55
F3	3 x 0.25	0.5 x 0.5	0.25 x 0.55
F4	3 x 0.25	0.7 x 0.7	0.25 x 0.55
F5	3 x 0.25	0.7 x 0.7	0.25 x 0.55
F6	3 x 0.25	0.7 x 0.7	0.25 x 0.55

3.3.1 Beam Element

The dimensions are selected according to TEC and TS500 resulting in 55cm depth and 25 cm width. Clear cover is selected as 2.5cm. Beam element is modeled in OpenSEES by using nonlinear force-based frame element and fiber discretization of the section. Using the fiber section model, unconfined region is defined and beam is meshed into 10 x 10 pieces.

In Figure 3.4, the gross sectional dimensions and the amount of longitudinal reinforcement in the beam elements are given. F1, F2, F3 type of frames uses type 1 beams and F4, F5, F6 type of frames uses type 2 beams. Unconfined region of the beam element is shown in Figure 3.4. In the design phase the beams are

supposed to be safe against shear failure, thus, sufficient shear reinforcement (stirrup) is supplied for beams. In Figure 3.4, the detail of reinforcement is given for support region of beam. The description of the concrete stress-strain relation for the unconfined region is presented in the Material Properties Section coming ahead in this chapter.

In OpenSEES (Mazzoni, McKenna, Scott, Fenves, 2009), fiber-based nonlinear beam-column element (Taucer, Spacone, Filippou, 1991) is the fundamental tool used for the nonlinear analysis of framed structural systems. The nonlinear response of this element is mainly derived by the integration of the material stress-strain relations over each section, and then the accumulated section responses give the force-deformation response of the element by using force-based shape functions. Force-based beam elements are now popularly used in research due to their accuracy and robustness in the nonlinear analysis of framed structural systems. In OpenSEES, by using the facility of fiber-based nonlinear beam-column element, unconfined and confined sections can be defined over the cross-section of a beam. Moreover, longitudinal reinforcements can be defined in the same way (See Figure 3.4).

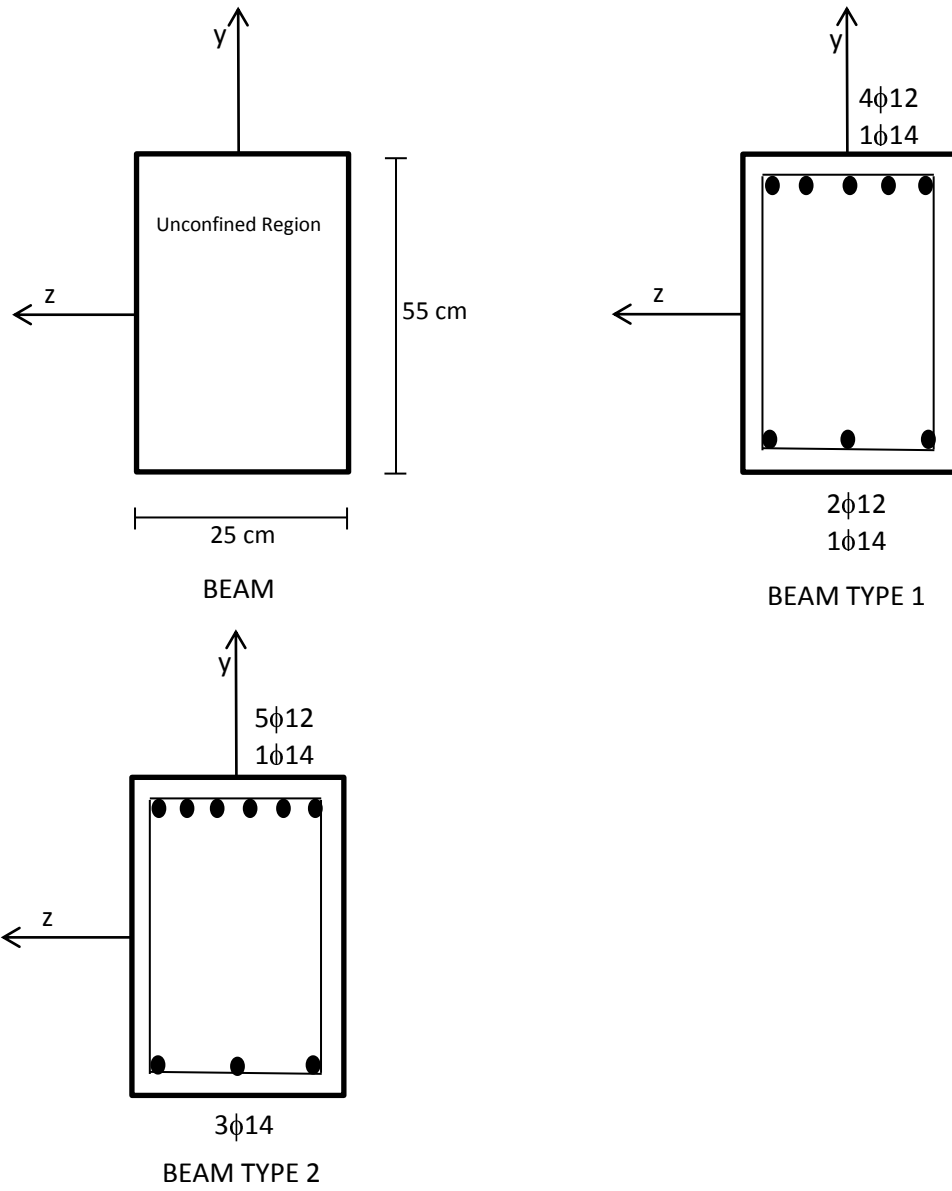


Figure 3.4 Sectional Dimension of Beams

3.3.2 Column and Shear Wall Elements

The dimensions of the column and wall elements are selected according to TEC and TS500. Clear cover is taken as 2.5cm. Fiber sections are used in OpenSEES for nonlinear modeling. Confined and unconfined sections are shown in Figure 3.4.

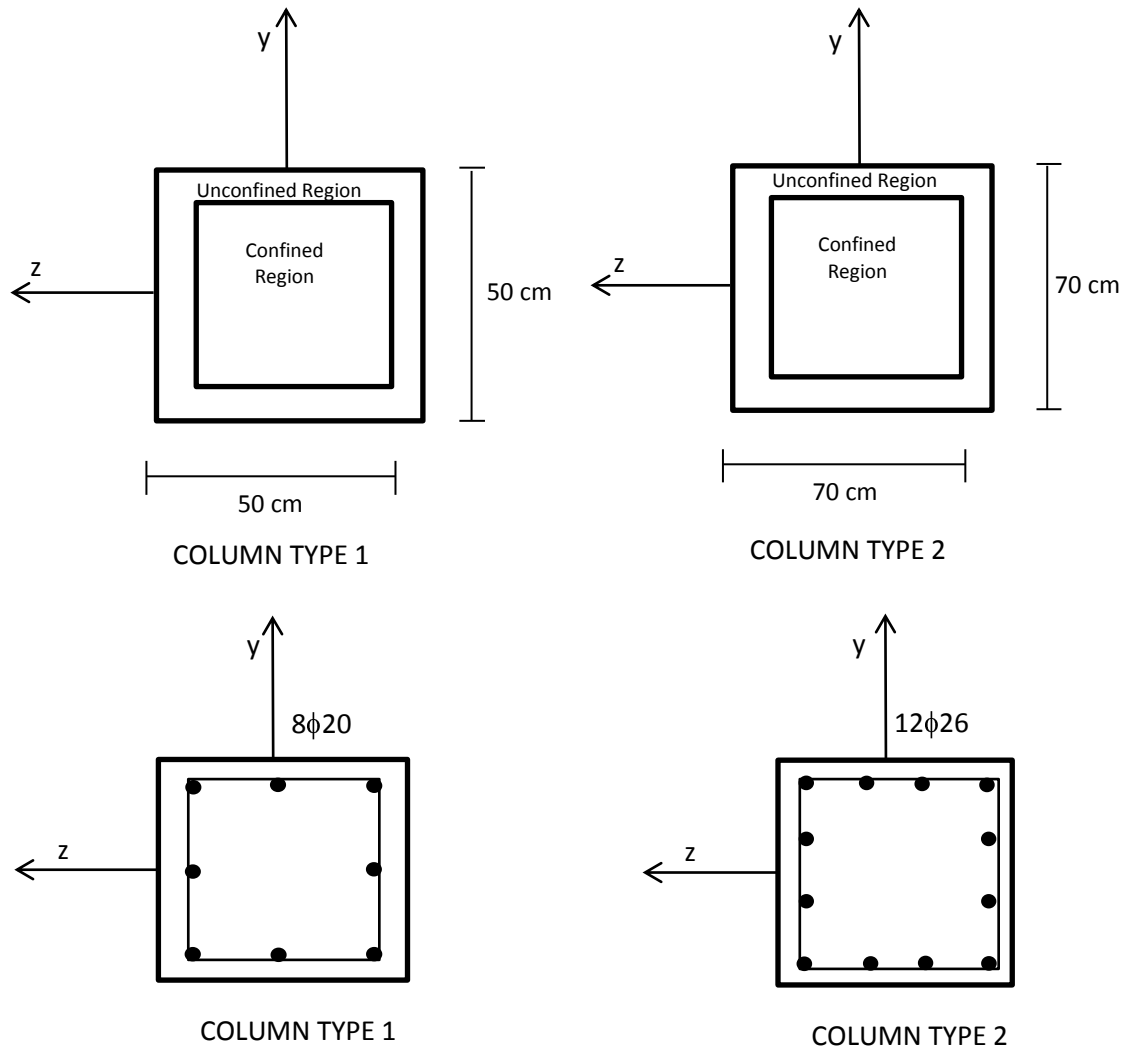


Figure 3.5 Dimensions of Columns

In Figure 3.5 two types of column are shown. Type 1 is used in buildings F1 to F3, and type two columns are used in buildings F4 to F6. These members are designed as high ductile.

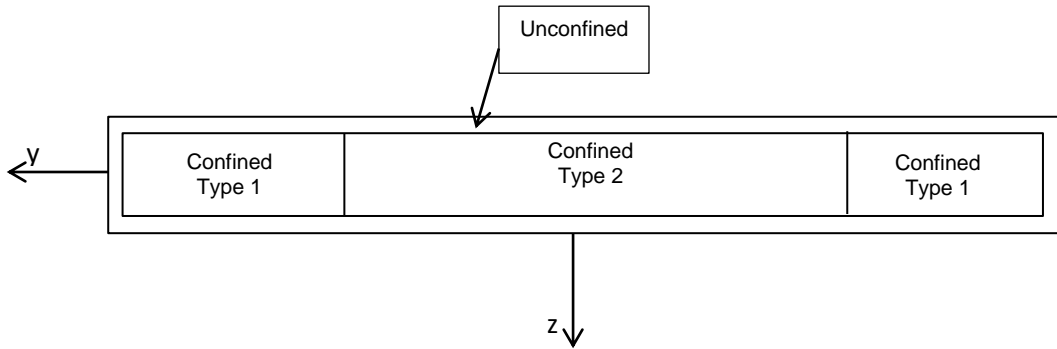


Figure 3.6 Regions in Shear Wall

Three types of material properties are used to describe the nonlinear material behavior of concrete in shear wall members (See Figure 3.6). Confined Type 1 has more confinement than other types. The concrete left out of the stirrups is assumed to compose the unconfined region (See Figure 3.8).

In Figure 3.7, the details of used walls are shown. For buildings F1 to F3 critical shear wall height is 6 m, and for buildings F4 to F6 critical shear wall height is 9 m. F1, F2, and F3 buildings contain wall type 1 under critical wall height and wall type 2 over critical wall height. Buildings F4, F5, and F6 use wall type 3 under critical wall height and wall type 4 over critical wall height. In the figure boundary zones are shown and its length changes from 40 cm to 60 cm. 2.5 cm concrete cover is used for the walls.

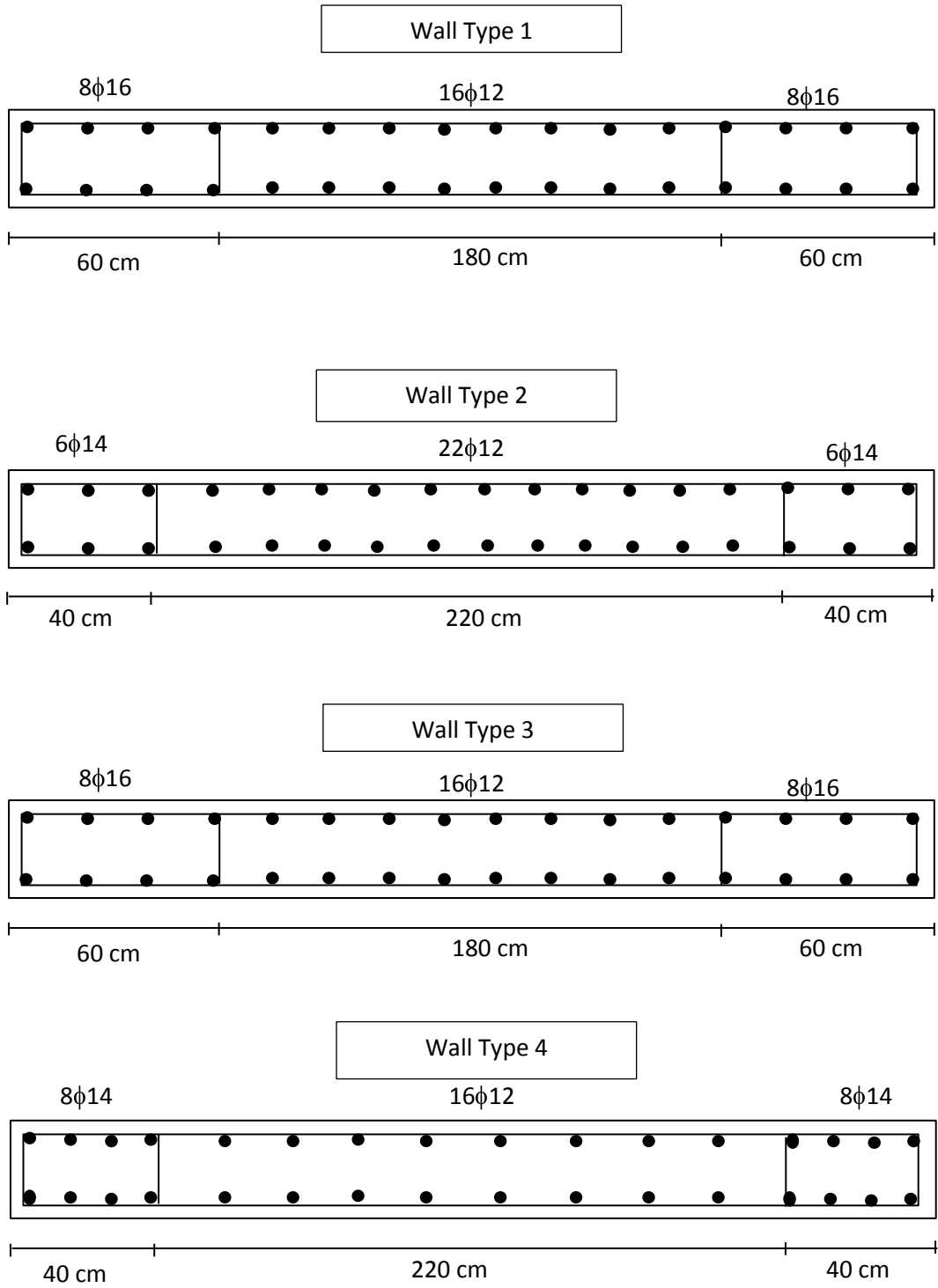


Figure 3.7 Details of Shear Wall

3.4 MATERIAL PROPERTIES

In OpenSEES, the concrete stress-strain relations can be defined as confined and unconfined with the use of appropriate material parameters, and furthermore the reinforcing steel can be defined as inelastic. The concrete model is selected as Concrete01 uniaxial material type (Mazzoni, McKenna, Scott, Fenves, 2007) and this model is based on Kent-Scott-Park material model (Kent, Park, 1971) with degraded reloading stiffness proposed by Karsan and Jirsa (Karsan, Jirsa, 1969) with an assumption of no tensile strength. The model requires compressive and crushing compressive strengths, and maximum and crushing strains to define the model. In Figure 3.8, concrete material model of Concrete01 object is shown. In this model concrete material has no tensile strength. In Figure 3.8, $\$epsU$ is ultimate strain, $\$epsc0$ is strain at peak compressive stress, $\$fpcu$ is ultimate stress and $\$fpc$ is peak compressive stress. Equation 3.1 gives the initial elastic modulus of the material model. For unconfined materials $\$fpcu$ parameter is set to zero.

$$E_i = 2 \times \frac{\$fpc}{\$epsc0} \quad 3.1$$

In all stages of the modeling, compressive strength of concrete is taken as 30 MPa. Detailed material parameters for columns and beams are written in the next, where the material properties are taken from the study conducted by Orakcal and Wallace (2006). For the columns, confined concrete has 0.002 strain at maximum compressive strength and ultimate strain is 0.012. Maximum compressive strength is 30 MPa and over ultimate strain columns continue to carry a compressive strength of 6 MPa. Moreover, unconfined concrete has 0.002 strain at maximum compressive strength and ultimate strain is 0.012. Over ultimate strain, the unconfined material regions of the columns carry no stress. For the beams, only unconfined concrete is used over the whole section, where the stress-strain relations are similar with the unconfined regions of the columns.

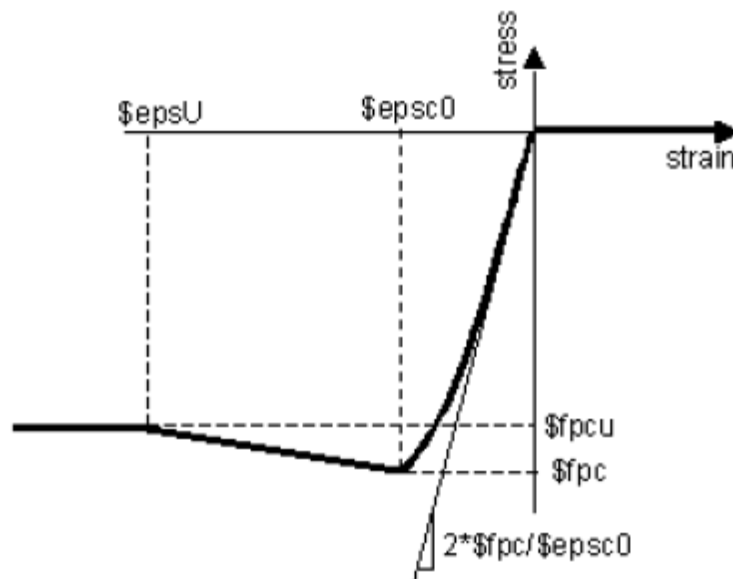


Figure 3.8 Concrete01 Material Model (Mazzoni et al., 2007)

For the shear walls, three types of material parameters are used as shown in Figure 3.6. In this figure, the confined type 1 concrete has 0.003 strain at maximum compressive strength and 0.020 ultimate strain. At ultimate strain wall has compressive strength of 18 MPa. The confined type 2 concrete has 0.002 strain at maximum compressive strength and 0.014 ultimate strain. At ultimate strain wall has compressive strength of 4.5 MPa. Furthermore, unconfined region of wall has 0.002 strain at maximum compressive strength and 0.008 ultimate strain. Over ultimate strain unconfined regions carry no stress. The calibration of these material properties falls in line with the methodology presented by Orakcal and Wallace (2006).

The reinforcements in the elements are modeled as single steel fibers across the section and this model uses Steel02 material model (Mazzoni et al., 2007). Steel02 material model uses a uniaxial Giuffre-Menegotto-Pinto steel material object with isotropic strain hardening (Mazzoni et al., 2007). In Figure 3.9, basic description of steel02 material model is presented. In this figure, E is the initial

elastic modulus, E_p is plastic modulus and R parameter controls the transition between elastic and plastic envelopes of the graphic. In the analysis R is selected 15. The yield stress of steel set to 420 MPa and initial elastic modulus is 200 GPa. Strain hardening ratio is 0.02 and isotropic hardening properties are set to default values (Mazzoni et al., 2007).

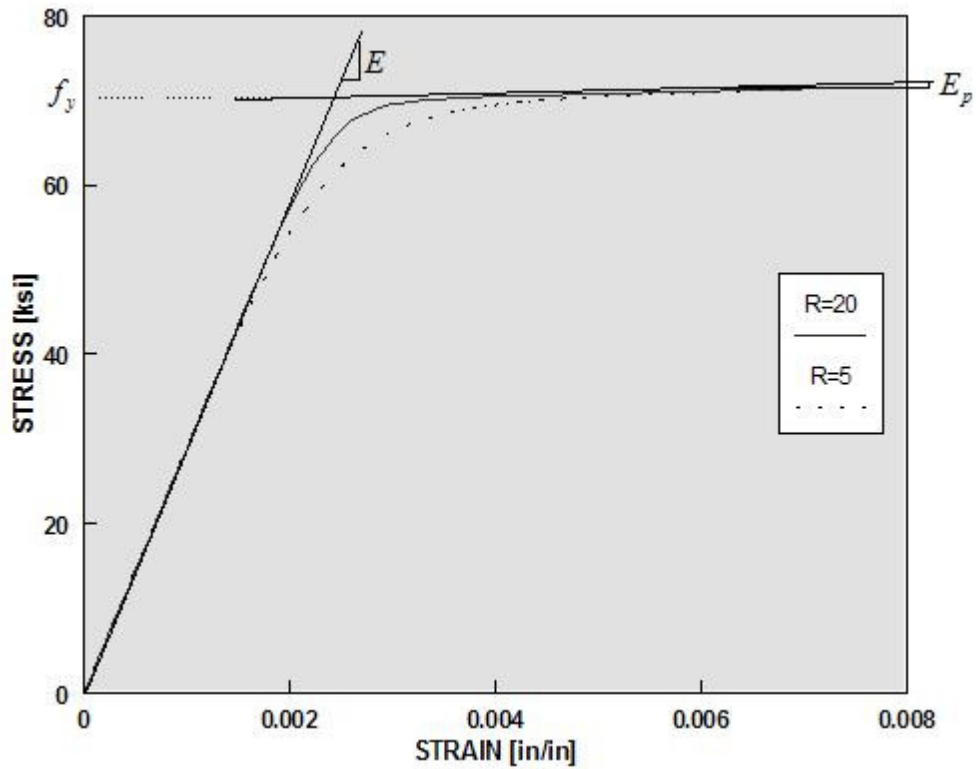


Figure 3.9 Steel02 Material Model (Mazzoni et al., 2007)

3.5 OpenSEES

Open System for Earthquake Engineering Simulation (OpenSEES) is an object oriented framework for finite element analysis. The software is an open source project, and program was developed by researchers at University of California, Berkeley for research purposes in advanced nonlinear finite element analysis.

OpenSEES has three parts, i.e. Modelbuilder, Domain, and Analysis, and in addition Recorder part exists. The main objects are controlled by Domain and other objects control the implementation of the analysis. OpenSEES has a powerful material, element and analysis libraries for the simulation of nonlinear models. Tcl scripting language is supported for powerful analysis organization (Mazzoni et al., 2007).

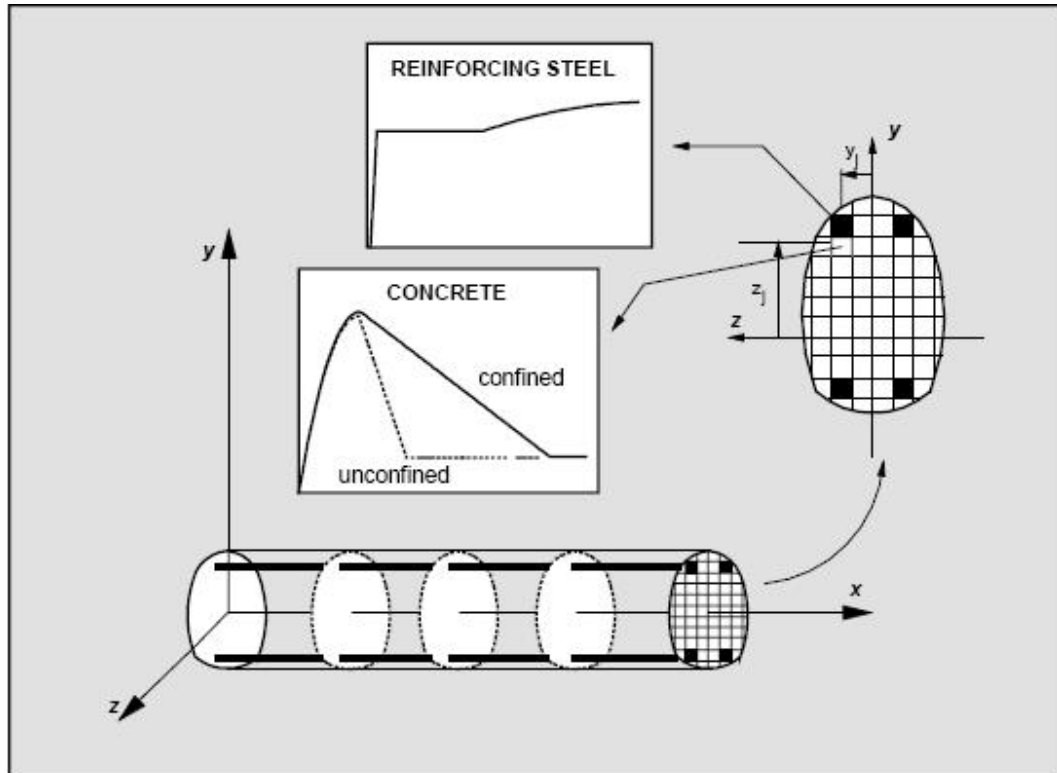


Figure 3.10 Fiber Discretization of Beam-Column Element (Taucer et al., 1991)

Taucer et al. (1991) developed a nonlinear force-based beam-column element using fiber discretization of the section. The force-based or also called as flexibility-based beam element is widely used for nonlinear analysis in research, and OpenSEES uses this model as its main frame element with nonlinear capabilities. In the model, the element is divided into longitudinal fibers and the model uses integration of the response of the fibers by considering uniaxial stress-

strain relation of the particular material (See Figure 3.10). The basic assumptions of the model are based on the small displacements and deformations and assumption of the plane sections remain plane. Moreover, the deformations due to shear and torsion are ignored in the model. For the recommended analyses, the integration points along the element length are set to five and the subdivisions along the section is based on fiber discretization (Taucer et al., 1991).

3.6 SCALING AND SELECTION OF GROUND MOTIONS

Traditional building design methods are code based methods and mostly elastic analyses are used for design of the building. However, nowadays performance based procedures are chosen for the evaluation of the performance of existing buildings. Most used methods are nonlinear static procedures for performance assessment of the building, but nonlinear time history analysis is also frequently employed. In the latter approach, selection and scaling of ground motions are taken into consideration in order to reduce the amount of computation that could be caused by using hundreds of unscaled ground motions. In this regards, ground motion selection can become the most important factor that affects nonlinear time-history analyses. Therefore, to gain responses of same order of magnitude from different ground motions, ground motions should be scaled for the median response of the buildings under different ground motions. For scaling two major methods are used: spectrum matching and amplitude scaling. Amplitude scaling has disadvantages because the method is good for fundamental period responses, but it has different responses for higher inelastic modes. To eliminate this drawback spectrum matching methods are developed by Abrahamson (Reyes, Chopra, 2011).

Eight individual ground motions are selected in this study from Strong Ground Motion Database of Pacific Earthquake Engineering Research Center (PEER) and their important properties are given in Table 3.4. For scaling the ground motions

spectrum match method is used. Scaled ground motions are generated by using the Rspmatch program developed by Abrahamson (Reyes, Chopra, 2011). Eight set of ground motions are scaled to the elastic design spectrum suggested by TEC. Scaled and unscaled spectra are shown in Figure 3.12 and Figure 3.11.

Table 3.4 Properties of Employed Ground Motions

Name	Earthquake	Country	Date	Location	Mw	PGA (g)	Site Condition
Gm1	Kocaeli	Turkey	17.08.1999	Düzce	7.4	0.348	CWB(D) USGS(C)
Gm2	Kocaeli	Turkey	17.08.1999	Düzce	7.4	0.535	CWB(D) USGS(C)
Gm3	Imperial Valley	California	15.10.1979	El Centro Array #1	6.5	0.139	CWB(D) USGS(C)
Gm4	Imperial Valley	California	15.10.1979	El Centro Array #12	6.5	0.143	CWB(D) USGS(C)
Gm5	Loma Prieta	California	18.10.1989	Waho	6.9	0.370	CWB(D) USGS(C)
Gm6	Friuli	Italy	06.05.1976	Tolmezzo	6.5	0.351	CWB(B) USGS(NA)
Gm7	Chalfant	California	20.07.1986	Zack Brothers Ranch	5.9	0.285	CWB(D) USGS(NA)
Gm8	Coalinga	California	22.07.1983	CHP 46T04	4.9	0.202	CWB(D) USGS(C)

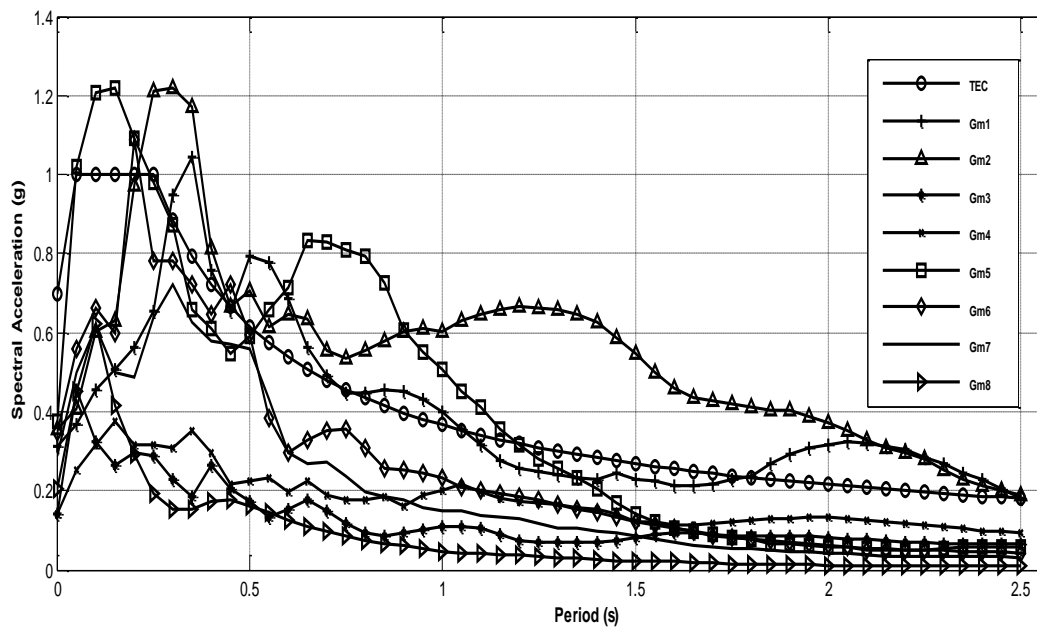


Figure 3.11 Spectral Acceleration vs. Period for Unscaled Ground Motions (5% Damped)

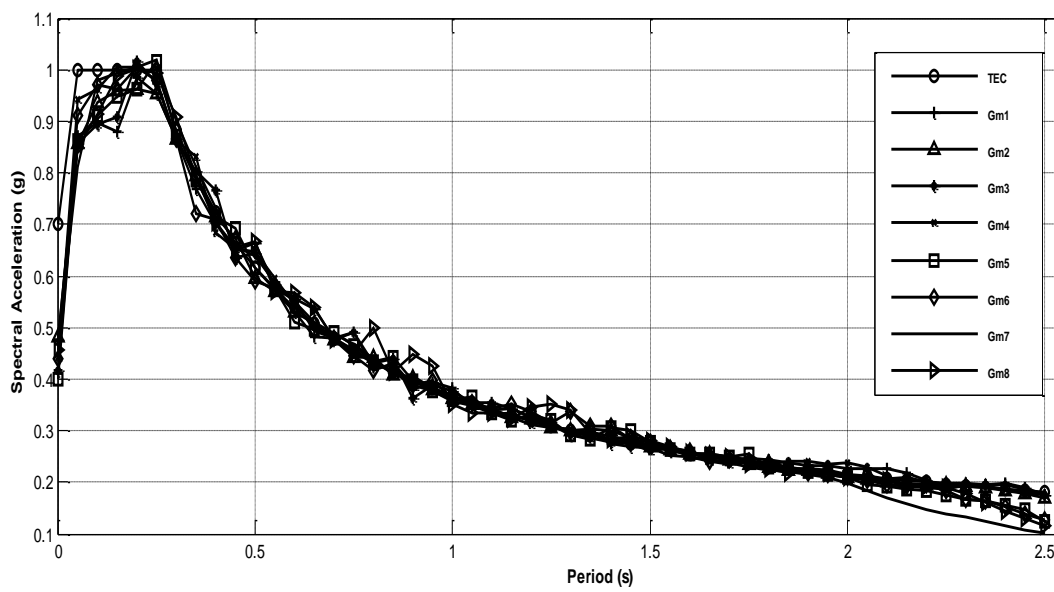


Figure 3.12 Spectral Acceleration vs. Period for Scaled Ground Motions (5% Damped)

3.7 RSPMATCH

Rspmatch is developed by Abrahamson in 1993. Rspmatch iteratively adjusts the original earthquake record to a target spectrum in time domain. The program can add wavelets having specified period ranges and limited durations to the input ground motion for scaling. This method is also called non-stationary spectrum matching method. The algorithm firstly developed by Lilhanand and Tseng and then Abrahamson modified the algorithm and developed Rspmatch program (Fahjan, Ozdemir, 2008). In analysis no filtering is used and twenty iterations are appropriate for matching the ground motion to the spectrum advised by TEC.

CHAPTER 4

RESULTS AND DISCUSSION

4.1 INTRODUCTION

In this chapter, nonlinear pushover and nonlinear dynamic analyses of the buildings described in the previous chapter are presented. These buildings are assumed to resist lateral loads in their own planes. In this regard, the buildings are hypothetical buildings designed for the sake of the research conducted in this thesis.

Buildings are analyzed under nonlinear static and dynamic loadings in order to understand the interaction between the frame and wall components. The pushover analysis is conducted by considering triangular, uniform and first-mode lateral load patterns presented in Figure 4.1. Nonlinear time-history analyses are utilized with scaled earthquake motions as mentioned in Chapter 3. To use the advantages of planar analysis lumped frames are used in two dimensions so that the behavior of nonlinear interaction between wall and frame can be investigated better. Moreover, lumped frames give the chance of better parametric study, because the computational burden can be minimized. For analysis OpenSEES finite element software package is employed due to its vast library of nonlinear models available for earthquake simulation of frame structural systems. OpenSEES can provide outputs that consist of member forces, drift ratios and plastic rotations of the selected frames. Among these results, particular ones are selected to be presented

in this chapter to discuss frame-wall interaction for the buildings having different height and different framing.

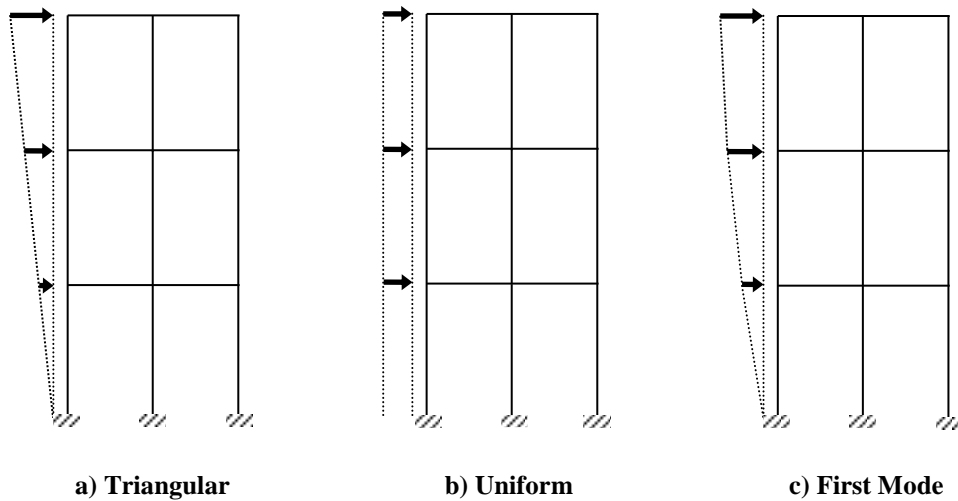


Figure 4.1 Applied Static Lateral Load Patterns

4.2 STATIC PUSHOVER ANALYSES

The pushover curves, plastic rotations, inter-story drifts and member forces of the 10-story buildings F1, F2, F3, and 15-story buildings F4, F5, F6 are presented through Figure 4.2 to Figure 4.21. The difference between the same story buildings (e.g. F1 and F2) is due to the percentage of base shear force carried by the wall in the design phase described in Chapter 3 (Please refer to Table 3.2).

The pushover results of the buildings F1 through F6 are presented in Figure 4.2 to Figure 4.4. In these figures, total base shear of the buildings and drift of top story are compared.

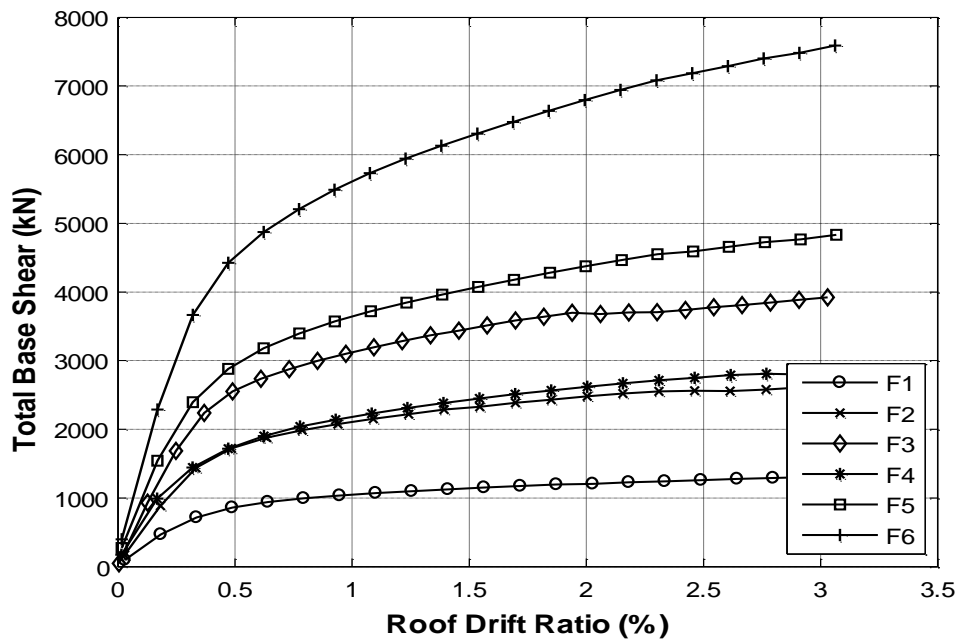


Figure 4.2 Total Base Shear vs. Roof Drift Ratio – Triangular Pushover Analysis

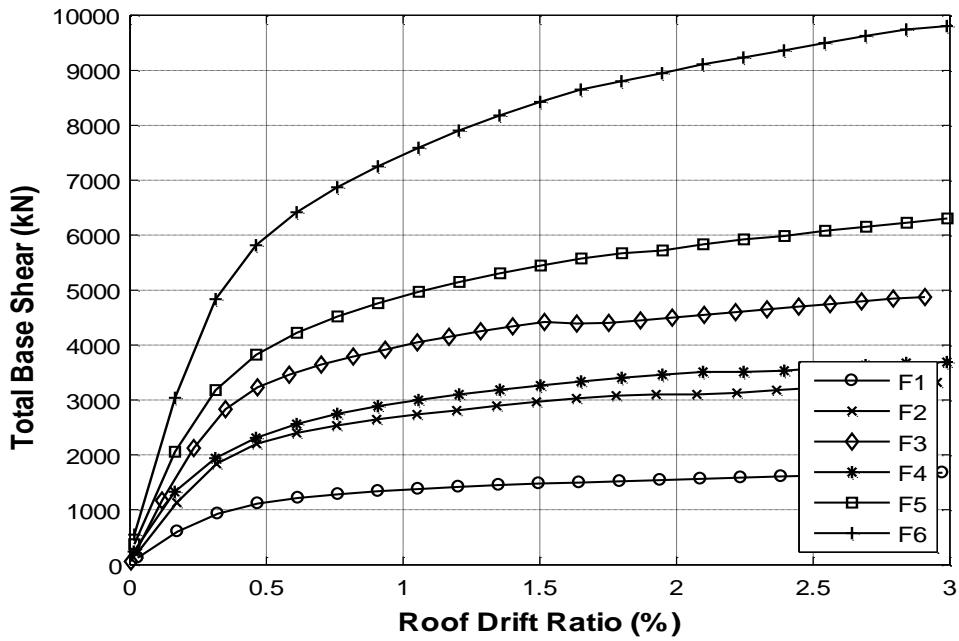


Figure 4.3 Total Base Shear vs. Roof Drift Ratio – Uniform Pushover Analysis

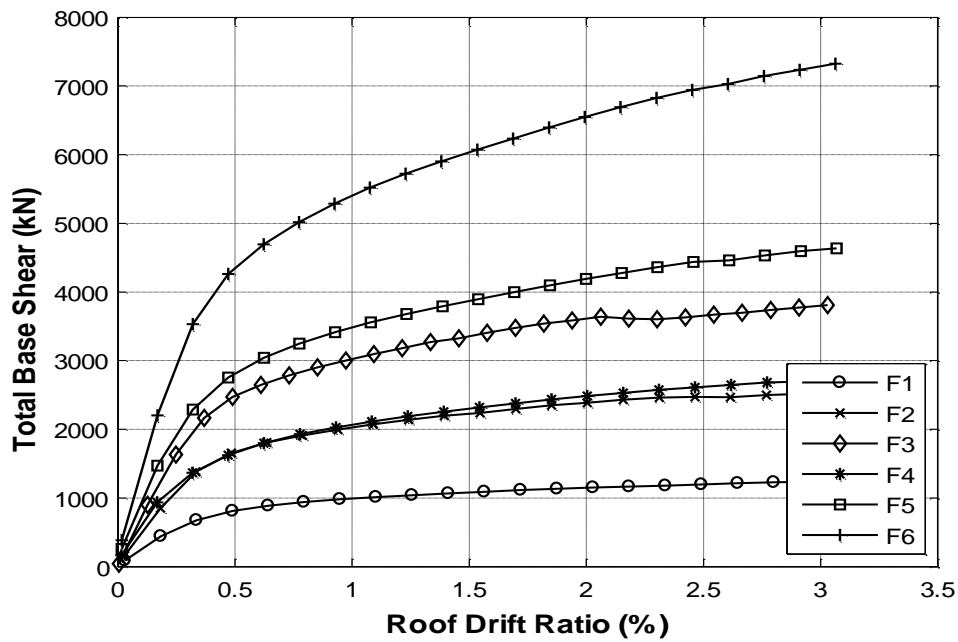


Figure 4.4 Total Base Shear vs. Roof Drift Ratio – First-Mode Pushover Analysis

Through Figure 4.2 to Figure 4.4, F1, F2 and F3 have 10 stories, and the lateral stiffness of F1, F2 and F3 increases as the base shear ratio of wall decreases. In the same way, F4, F5 and F6 have 15 stories, and the lateral stiffness of F4, F5 and F6 increases as the base shear ratio of wall decreases. The 15-story buildings are stiffer than 10-story buildings because the member sizes of 15-story buildings are larger. In addition, the triangular and first-mode lateral load cases yield similar results. After 0.5% roof drift ratio, nonlinear behavior of buildings are observed due to the inelastic action in the walls. Thus, the nonlinear behavior of frame-wall type buildings mainly starts as a result of the nonlinearity in the walls. After 0.5% roof drift ratio, the buildings perform stable nonlinear behavior even when the wall appears to soften, because the redistribution between wall and frame provides the required strength to keep the building's response ductile. In three lateral loading cases, uniform loading case punishes the building more than triangular and first-mode lateral loading cases so that the building have to resist more lateral load in uniform loading.

4.2.1 Pushover Results of Selected Elements

Roof drift ratio of wall and columns are given through Figure 4.5 to Figure 4.10. These figures give detailed information about interaction between wall and columns.

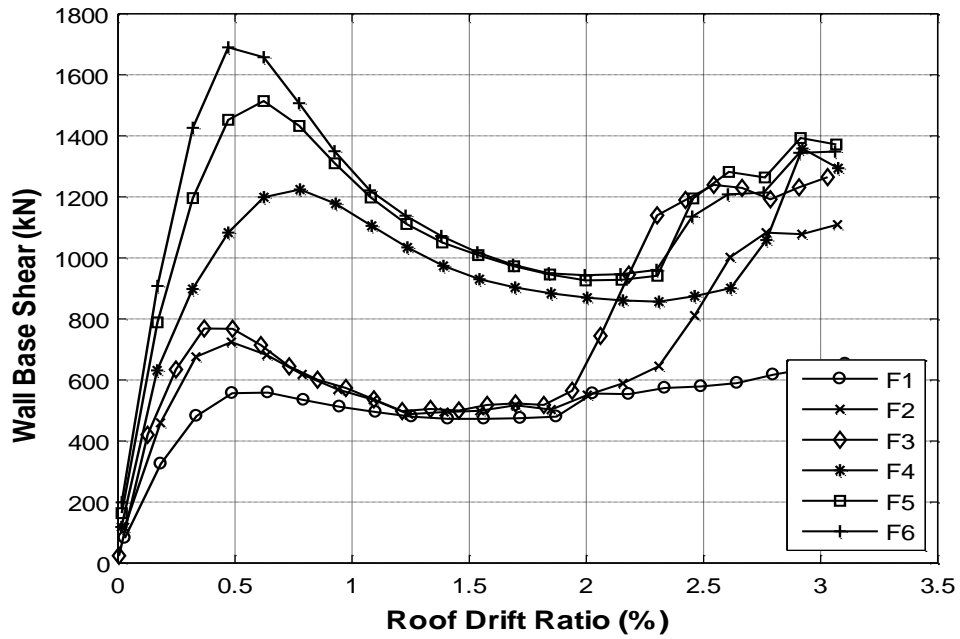


Figure 4.5 Wall Base Shear vs. Roof Drift Ratio – Triangular Pushover Analysis

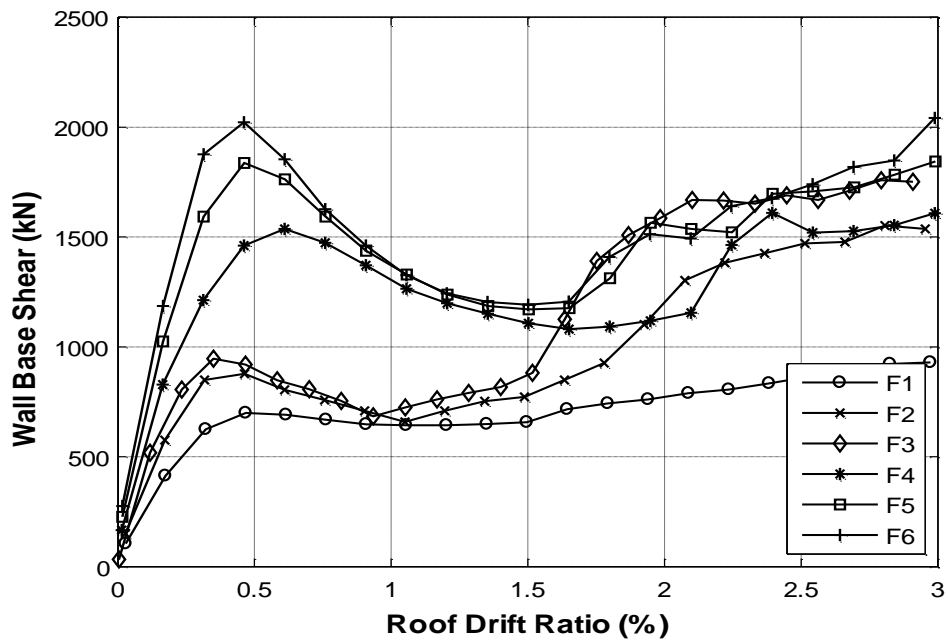


Figure 4.6 Wall Base Shear vs. Roof Drift Ratio – Uniform Pushover Analysis

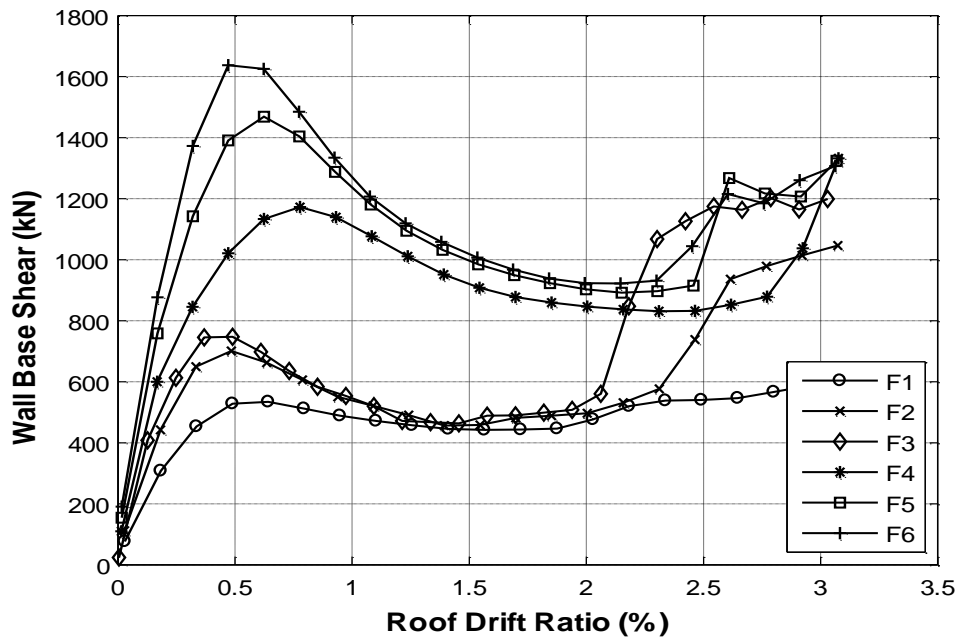


Figure 4.7 Wall Base Shear vs. Roof Drift Ratio – First-Mode Pushover Analysis

The shear force carried by the walls is presented through Figure 4.5 to Figure 4.7. The lateral stiffness increases as the base shear ratio of wall decreases in above figures. The 15-story buildings are stiffer than the 10-story buildings because the member sizes and reinforcements of wall of 15-story buildings are larger than the 10-story buildings. In addition, the triangular and first-mode lateral load cases yield similar results for the wall. After 0.5% roof drift ratio, the wall appears to soften more especially when the height of the building increases. We believe that this is caused by the redistribution of forces between the wall and frame components. It is worth to mention that the wall performs stable ductile performance when it is analyzed by itself alone in OpenSEES (i.e. not connected to the columns as part of the analysis conducted in F1 to F6 buildings). During that stand-alone analysis, the wall shows significant nonlinearity due to yielding at 0.5% roof drift ratio, as well, but no softening in the response was observed after that point. Once again coming back to the results of F1 to F6 buildings, columns start yielding around 1.5% roof drift ratio, and the walls provide the necessary capacity for the ductile response of the building after this incidence. In three lateral loading cases, uniform loading case punishes the building more than triangular and first-mode loading cases so that the building have to resist more lateral load in uniform loading.

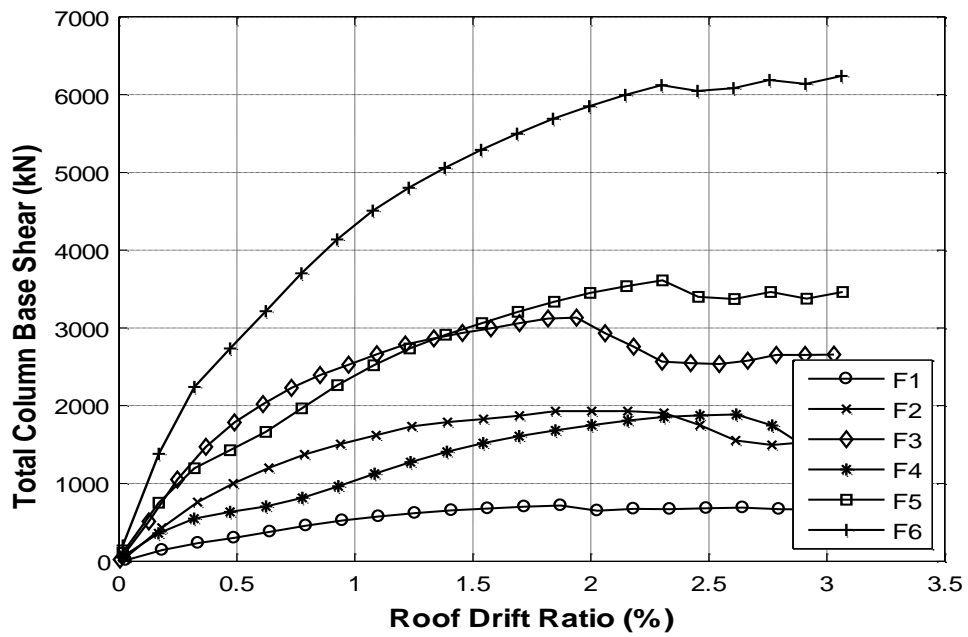


Figure 4.8 Total Column Base Shear vs. Roof Drift Ratio – Triangular Pushover Analysis

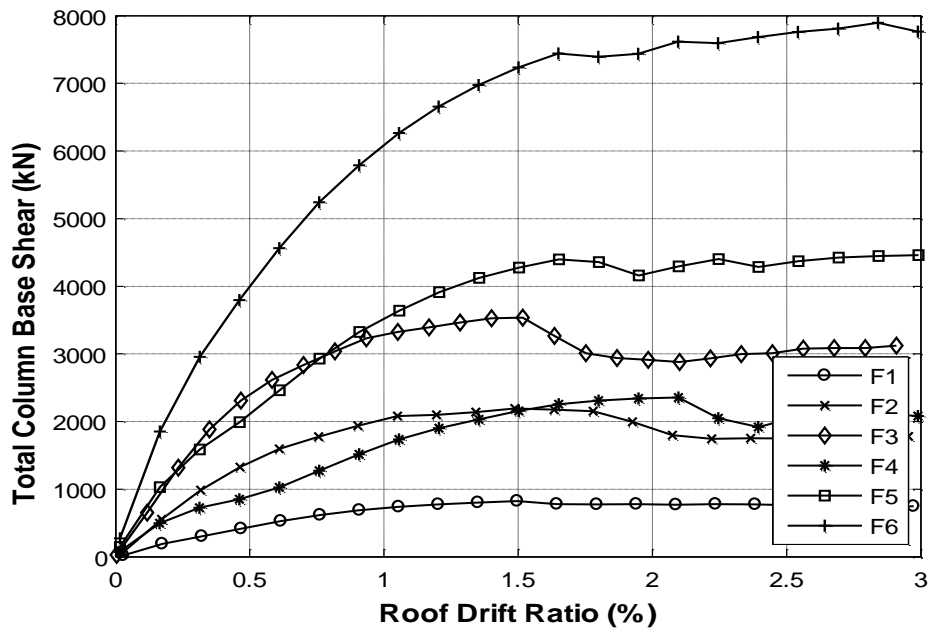


Figure 4.9 Total Column Base Shear vs. Roof Drift Ratio – Uniform Pushover Analysis

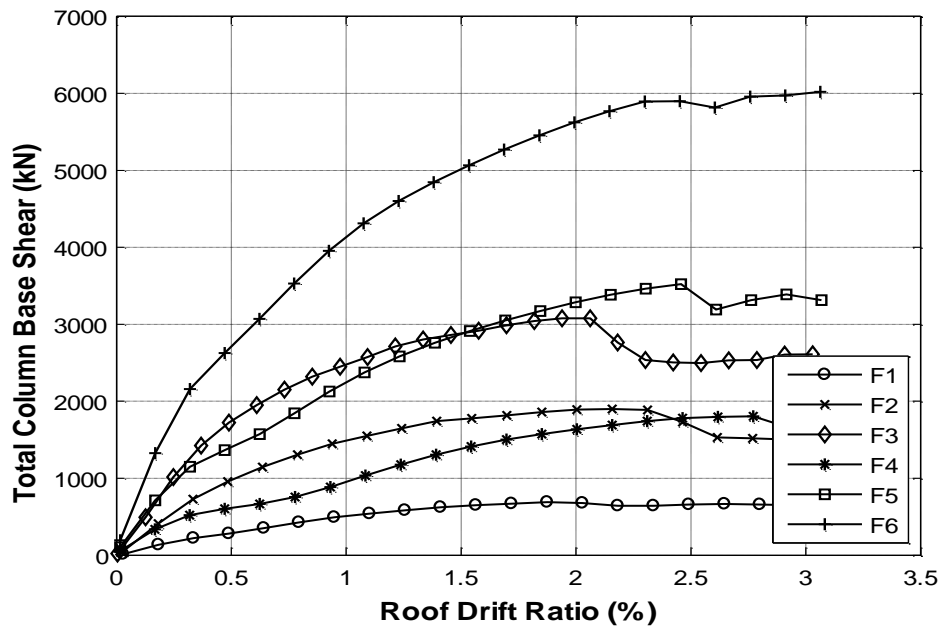


Figure 4.10 Total Column Base Shear vs. Roof Drift Ratio – First-Mode Pushover Analysis

The shear force carried by the columns is presented through Figure 4.8 to Figure 4.10. The lateral stiffness of total columns in a building increases as the base shear ratio of the wall of that building decreases. Moreover, the increase in building height raises the lateral stiffness of the building. The triangular and first-mode lateral load cases yield similar results for the columns. After 1.5% roof drift ratio, the columns start to crack, therefore, the wall starts to supply the necessary capacity for large drift of the building. F1 is the weakest building among all due to its design. It can be said that the uniform loading case punishes the columns more than other loading cases, because some columns starts to crack at lower drift ratio in uniform loading case.

Through Figure 4.2 to Figure 4.5, it is understood that the change in nonlinear behavior of the buildings started at 0.5% roof drift ratio and they showed ductile behavior under different loading cases. Through Figure 4.6 to Figure 4.8, the wall started to change its nonlinear behavior at 0.5% roof drift ratio, moreover, the

building started to yield at 0.5% ratio. Therefore the general nonlinear behavior of building was determined by wall. In addition, all walls started to change its nonlinear behavior at same roof drift ratio because the wall had constant width of 3m and same amount of drift caused the same amount of rotation for the wall and same amount of strain at the edge reinforcements of the wall. The nonlinear material properties are same in all reinforced concrete buildings, as a result, the wall yielded at same roof drift ratio. Therefore, it can be said that the nonlinear behavior of a frame-wall building depends on the width of the wall significantly. Once the wall lost its lateral strength, the columns supplied the required amount of strength to carry the lateral load in the analyses. Interestingly, after 1.5% roof drift ratio the columns started to crack and the walls started to supply the required strength for ductile response.

4.2.2 Plastic Rotation of Selected Elements

In this section, inelastic behavior of column and wall elements, maximum plastic rotations of wall and middle column (See Figure 3.1) are discussed under different lateral load patterns for detailed investigation of local response of the buildings.

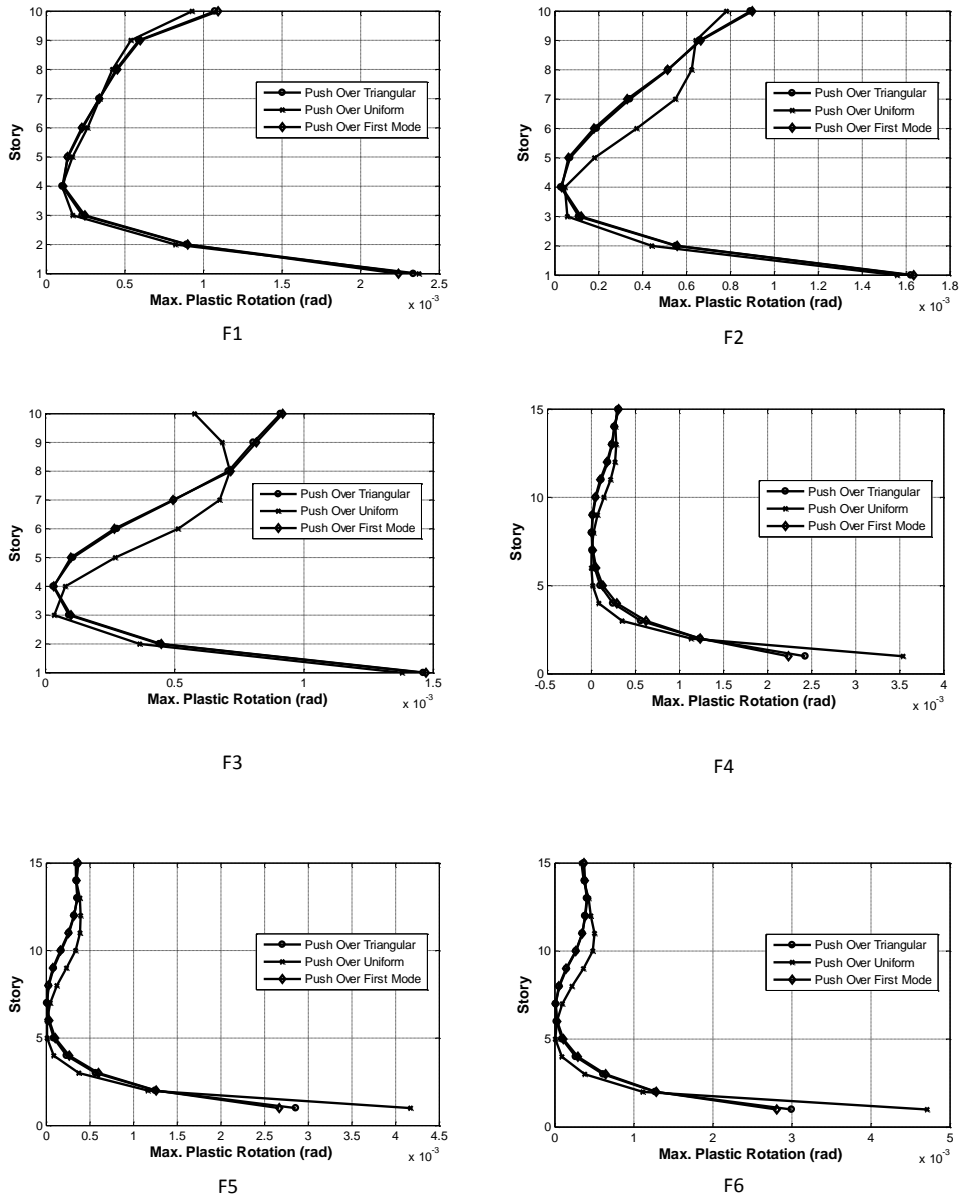


Figure 4.11 Story vs. Maximum Plastic Rotation for Middle Column – Pushover Analysis

In Figure 4.11, maximum envelopes of plastic rotations of the middle column (See Figure 3.1) of the buildings are given. In Figure 4.11, at the second story level, concentration in the plastic rotation is seen for all buildings. 15-story buildings have more plastic rotation at base level than 10-story buildings. Moreover, when

shear force ratio of the wall decreases, in other words, the lateral stiffness of building increases, the plastic rotation decreases in middle columns. Load cases do not change the plastic rotation particularly in F1, F4, F5 buildings. However, in F2 and F3 buildings, uniform lateral load pattern produces slightly different result than other lateral load pattern. 10-story buildings F2 and F3 have 57.13 %, 46.5 % elastic base shear force ratio of wall respectively. The reason for the difference of plastic rotation in these buildings is not known clearly, but it can be said that the elastic base shear force ratio of wall can affect the plastic rotations of wall in uniform lateral load pattern.

In Figure 4.12, maximum envelopes of plastic rotations of the wall of the buildings are given. At second story, concentration in the plastic rotation is seen for all buildings. The plastic rotation of the wall is not affected due to the change in building height, because all buildings have 3 m width wall and the width of the wall influences the nonlinear property the most in these simulations. For 10-story buildings, at seventh story, plastic rotation increases, because the modal shape of the building affects the buildings nonlinear behavior. In the same way, for 15-story building, at tenth story, plastic rotation increases. Loading cases do not change the plastic rotation particularly except for F2 and F3 buildings. The same can be concluded for columns in terms of the difference in plastic rotations of wall for uniform lateral load pattern.

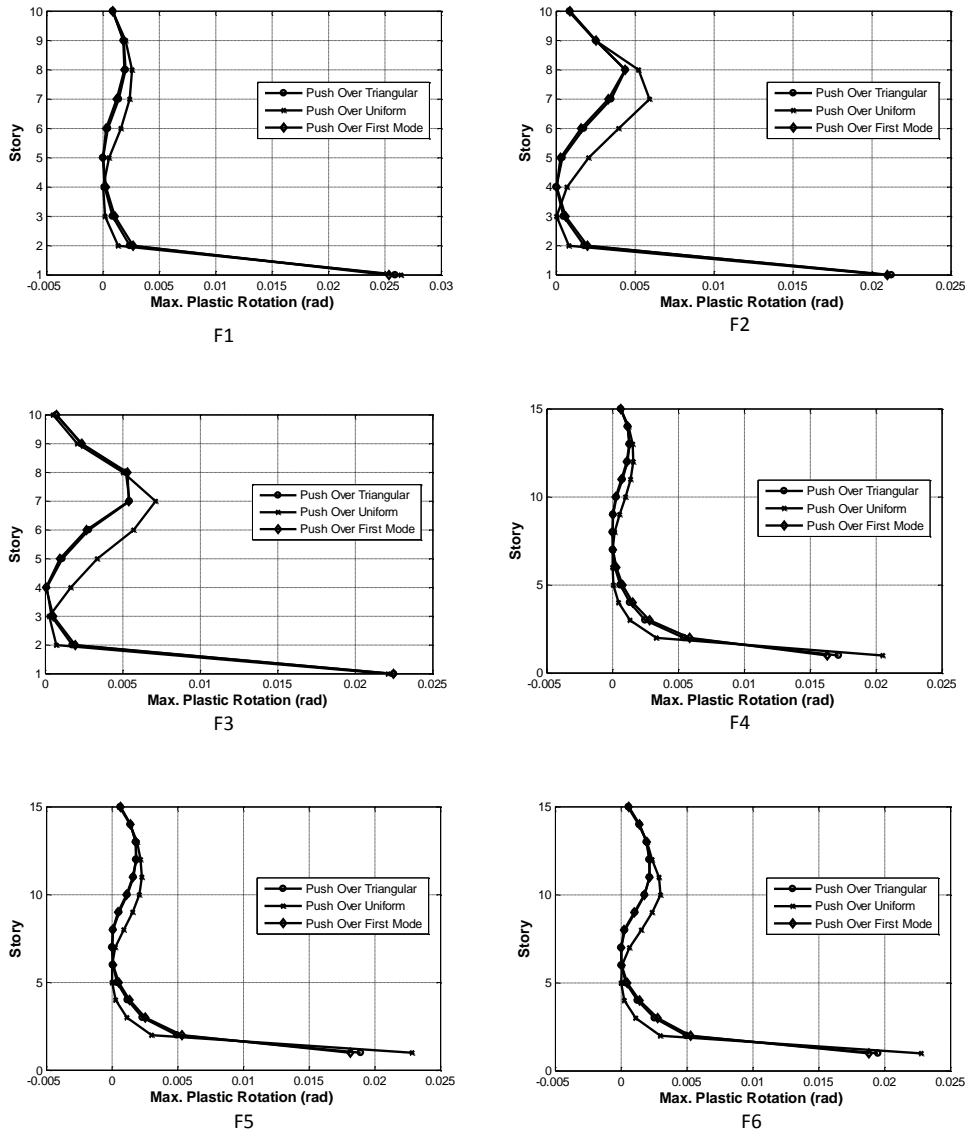


Figure 4.12 Story vs. Maximum Plastic Rotation for Wall – Pushover Analysis

To compare the differences of plastic rotations between wall and middle column, plastic rotations were not observed for wall at top story, but for columns there were significant plastic rotations. It can be said that there was not a direct relationship between the plastic rotations of wall and column. The height of building influenced the column particularly, but the wall was not affected from

the change of building's height. Base plastic rotations of middle column nearly doubled as the building height increased.

4.2.3 Inter-Story Drift

Inter-story drift is an important parameter to investigate for understanding the relationship between neighboring stories. It develops the displacement transition between stories. To understand these relationships, maximum envelopes of inter-story drift ratio of the buildings are given through Figure 4.13 to Figure 4.15.

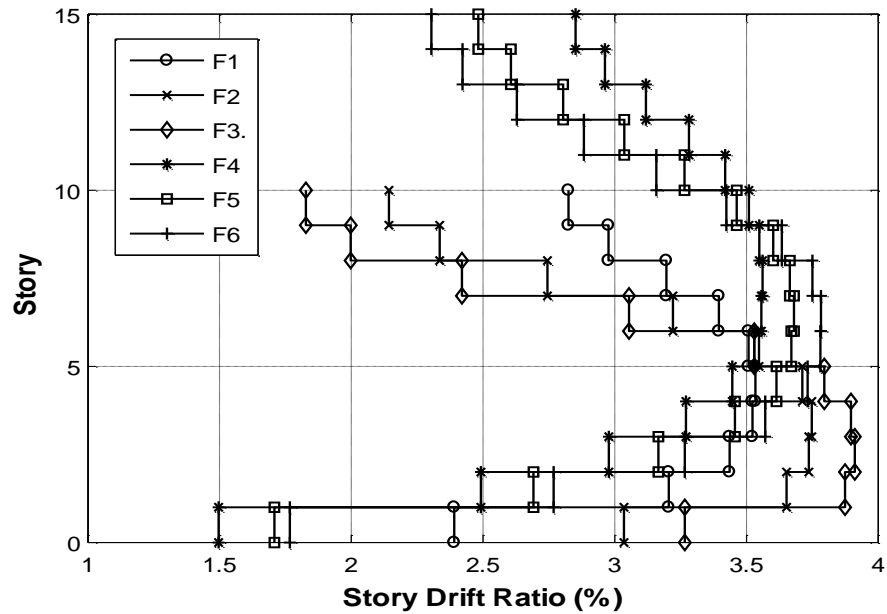


Figure 4.13 Story vs. Inter-Story Drift Ratio – Triangular Pushover Analysis

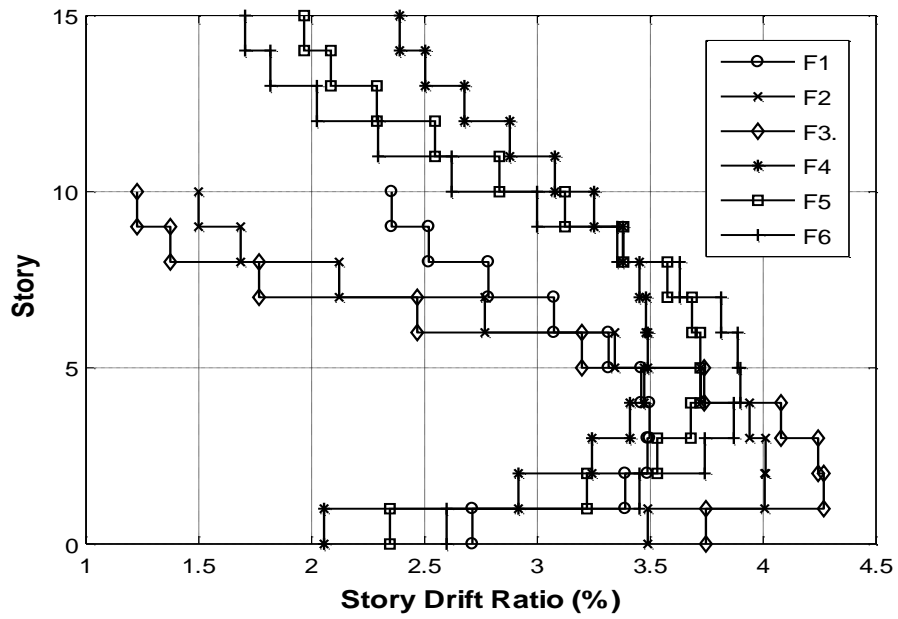


Figure 4.14 Story vs. Inter-Story Drift Ratio – Uniform Pushover Analysis

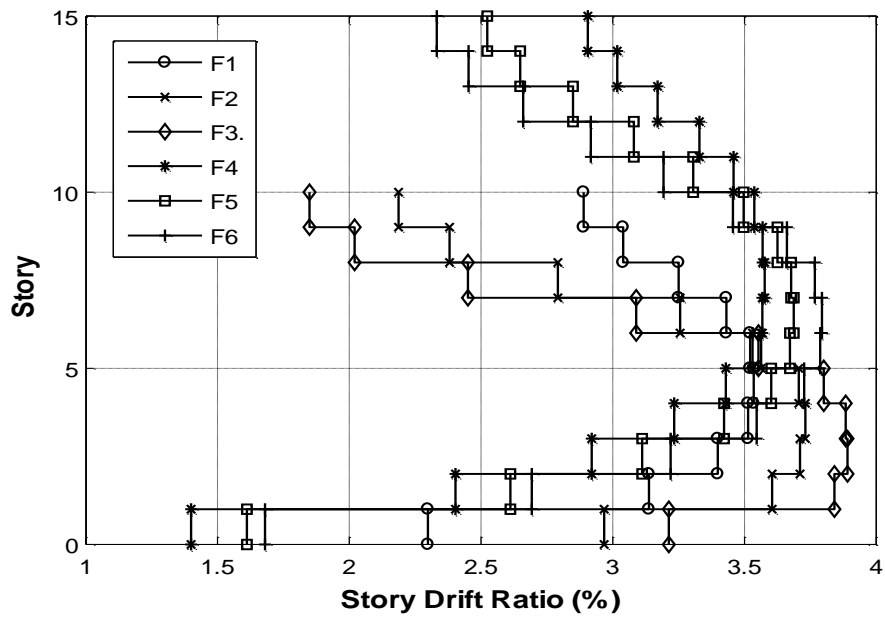


Figure 4.15 Story vs. Inter-Story Drift Ratio – First-Mode Pushover Analysis

Through Figure 4.13 to Figure 4.15, maximum envelopes of inter-story drift ratio of the buildings are given. From these figures, it is understood that inter-story drift

ratio is close to the results of other loading cases for the same building height. The loading case does not affect the inter-story drift significantly. Moreover, it is clear that the rapid change in inter-story drift ratio is observed at second story level for all buildings. While the base shear ratio of wall decreases, the inter-story drift ratio decreases at the stories near the top story and basement. At the middle stories, the changes in the base shear ratio of wall do not change the inter-story ratio of buildings. The increase in the height of building also increases the inter-story drift ratio.

4.2.4 Patterns of Static Load Effects

In this section, axial force, bending moment and shear force distributions along each column and wall at the end of the lateral load analyses are presented through Figure 4.16 to Figure 4.21. It is important to investigate the force levels between stories because they give the meaningful results for understanding the nonlinear force distribution among stories and between frame and wall components. To understand these relationships the static load effects are discussed in this section.

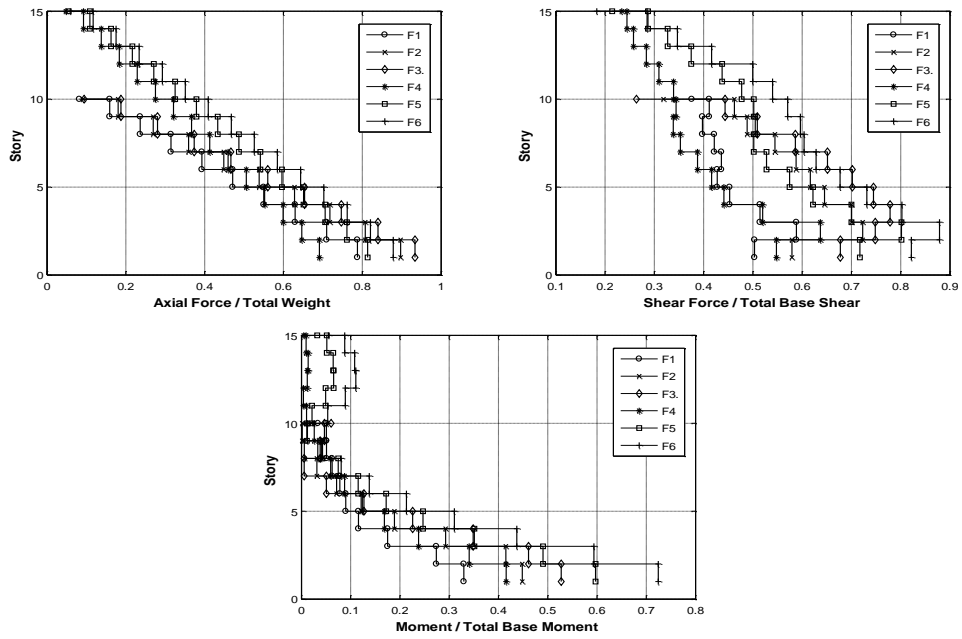


Figure 4.16 The Total Internal Force Distributions in Columns at the end of Triangular Pushover Analysis

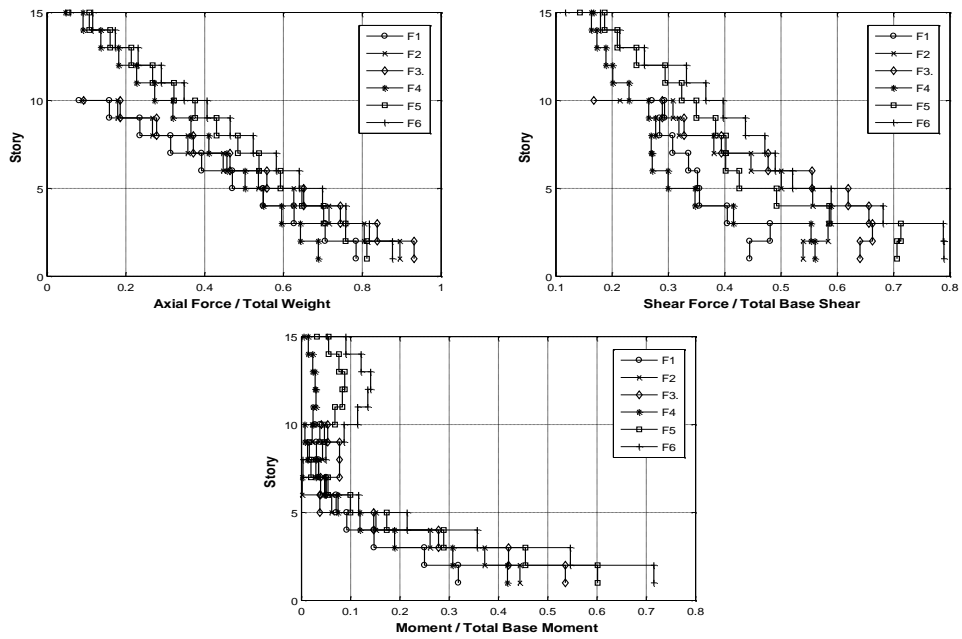


Figure 4.17 The Total Internal Force Distributions in Columns at the end of Uniform Pushover Analysis

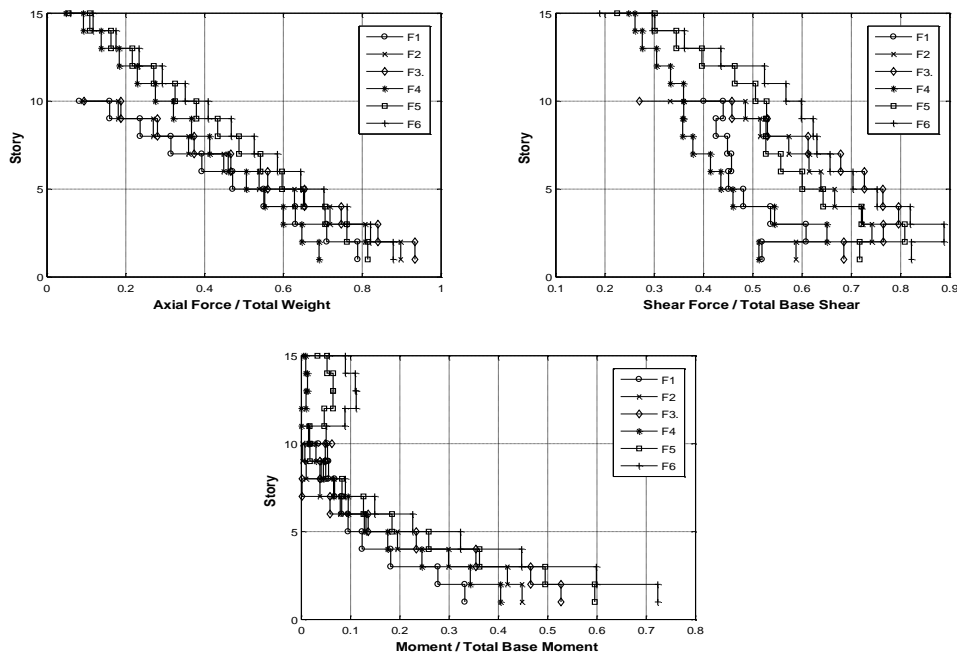


Figure 4.18 The Total Internal Force Distributions in Columns at the end of First-Mode Pushover Analysis

Through Figure 4.16 to Figure 4.18, different lateral load results are presented for columns at the end of the analyses corresponding to approximately 3% roof drift ratio. In these figures, it is understood that the buildings do not collapse under all loading cases, because axial load level of columns are adequate for the buildings to remain safe. In Figure 4.16, the base shear ratio of F1 building is 50% and base shear ratio of F6 building is 83% at triangular pushover analysis. In elastic analysis, F1 building has 25% base shear force ratio as mentioned in Chapter 3. These ratios are different from static analysis, because the nonlinear material property changes the behavior of the building significantly and at end of the analysis the columns have less damage than the walls so that the increase in the base shear ratio in columns is an expected situation. Moreover, it can be said that same situation are seen in Figure 4.17 and Figure 4.18.

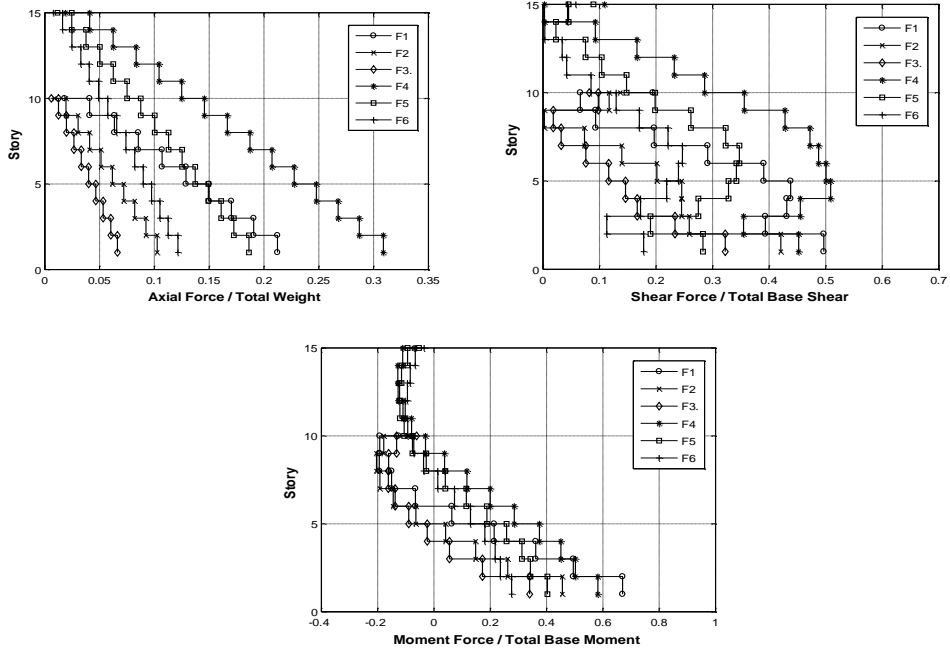


Figure 4.19 The Total Internal Force Distributions in Wall at the end of Triangular Pushover Analysis

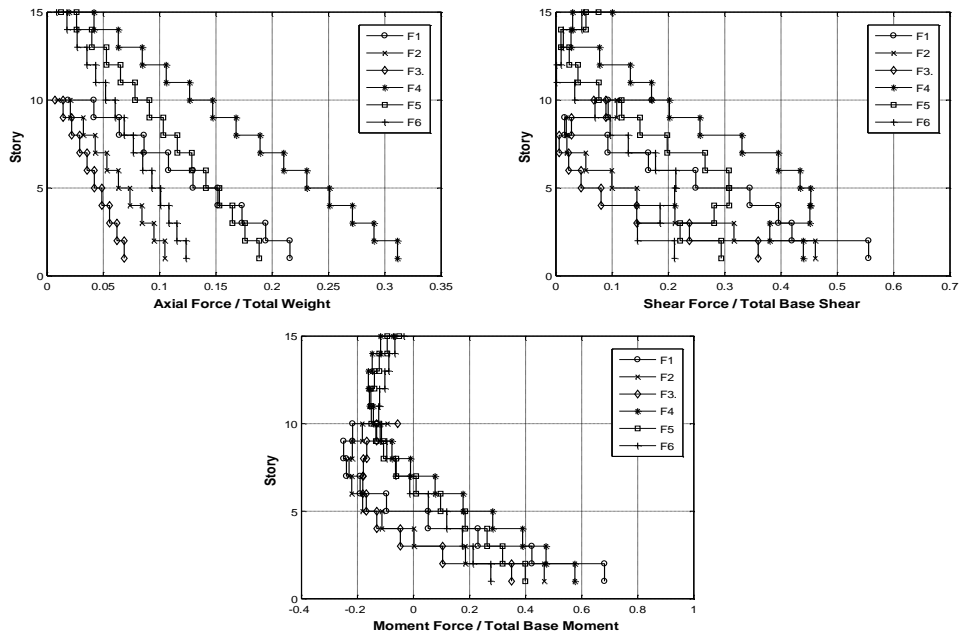


Figure 4.20 The Total Internal Force Distributions in Wall at the end of Uniform Pushover Analysis

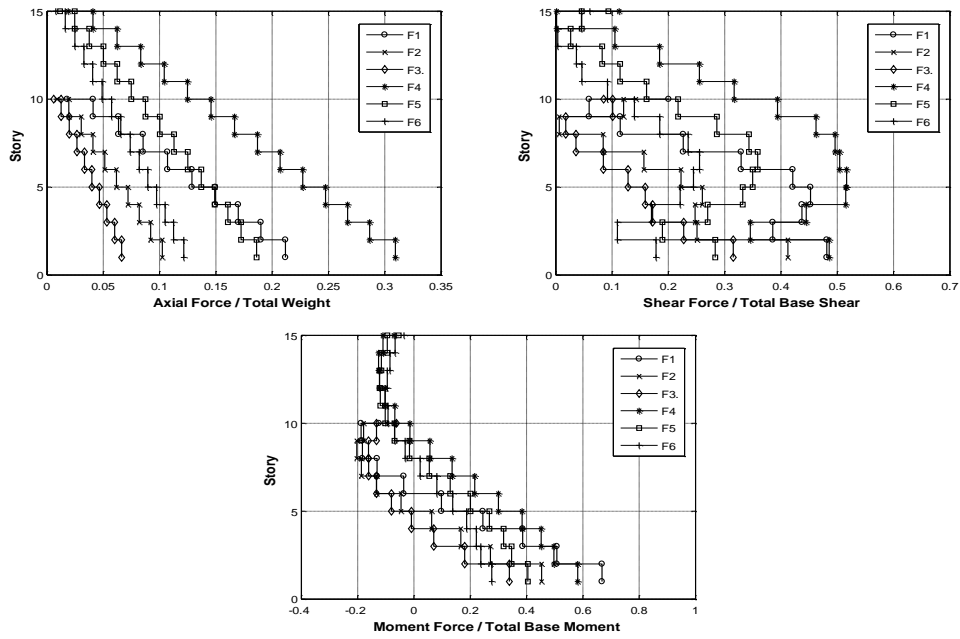


Figure 4.21 The Total Internal Force Distributions in Wall at the end of First-Mode Pushover Analysis

Through Figure 4.19 to Figure 4.21, different lateral load results are presented for wall at the end of the analyses. In these figures, like columns, wall remains safe under several lateral loading cases as axial load level of wall are adequate for the buildings. In Figure 4.19, base shear force ratio for wall of F1 building is 50% and base shear force ratio for wall of F6 building is 17% in nonlinear lateral load analysis. In elastic analysis, the base shear force ratio for column is higher than corresponding ratios in nonlinear lateral load analysis for columns so that the walls are weaker than the columns under nonlinear lateral load analyses.

4.2.5 Comparison of Wall Base Shear Ratio

In this section base shear force ratio of wall in elastic and inelastic analyses are given through Table 4.2 to 4.3. In these tables, the change in inelastic base shear force ratio of wall is compared with the designed value of the elastic base shear force ratio given in Chapter 3. The design was conducted by assuming gross

sectional properties as suggested by TEC 2007 and TS500. It is important to track the changes in this ratio because it gives information about the shear force distribution between wall and frame components.

Table 4.1 Comparison of Inelastic Base Shear Force Ratio of Wall at 0.0% Roof Drift Ratio

FRAME	Elastic Base Shear Force Ratio of Wall %	Inelastic Base Shear Force Ratio of Wall at 0.0% Roof Drift Ratio		
		Triangular %	Uniform %	First-Mode %
F1	75.2	83.2	81.3	83.4
F2	57.1	69.1	67.3	70.0
F3	46.5	57.2	57.9	57.1
F4	73.1	78.2	76.5	78.2
F5	57.7	64.2	64.9	64.2
F6	44.2	53.1	53.4	53.1

In Table 4.1, 10-story buildings F1, F2, F3 have elastic base shear ratio of wall changing between 75.2% and 46.5%. In the same way, 15-story buildings F4, F5, F6 have elastic base shear force ratio of wall changing between 73.1% and 44.2%. These percentages are selected from TEC for the limit design parameters. These parameters are captured from the analyses just after the analyses start namely it can be said that it is the beginning of the analyses. At the beginning of the analyses the inelastic base shear force ratio of wall is not significantly different for triangular, uniform, first-mode lateral load cases. However, there is a significant difference between elastic and inelastic base shear force ratio of wall because the nonlinear material has an higher initial tangent modulus and the force redistribution and cracked section parameters affect the inelastic base shear force ratio of wall. The increase in base shear force ratio between elastic and inelastic case does not depend on the total height of building because the increase in base shear force ratio is constant in all cases.

Table 4.2 Comparison of Inelastic Base Shear Force Ratio of Wall at 0.5% Roof Drift Ratio

FRAME	Elastic Base Shear Force Ratio of Wall %	Inelastic Base Shear Force Ratio of Wall at 0.5% Roof Drift Ratio		
		Triangular %	Uniform %	First-Mode %
F1	75.2	64.1	62.8	63.9
F2	57.1	41.2	39.8	41.9
F3	46.5	49.0	48.1	49.2
F4	73.1	63.1	63.9	63.2
F5	57.7	50.1	47.0	50.1
F6	44.2	38.2	34.2	38.3

In Table 4.2, the inelastic parameters are taken in the analyses at the 0.5% roof drift ratio. At this point, wall shows different nonlinear behavior and this nonlinearity affects the inelastic base shear force ratio. All lateral load patterns produces similar results, thus, it can be said that the inelastic base shear ratio of wall at the early stages of analyses is not affected from lateral load pattern. Additionally, the inelastic base shear force ratio of wall drops below the values corresponding to the elastic analyses and the decrease is constant for all buildings. Therefore, the change in inelastic base shear ratio of wall is not affected from the elastic base shear ratio of wall and total buildings height.

Table 4.3 Comparison of Inelastic Base Shear Force Ratio of Wall at 2.0% Roof Drift Ratio

FRAME	Elastic Base Shear Force Ratio of Wall %	Inelastic Base Shear Force Ratio of Wall at 2.0% Roof Drift Ratio		
		Triangular %	Uniform %	First-Mode %
F1	75.2	46.1	50.5	43.6
F2	57.1	22.3	36.5	21.2
F3	46.5	33.6	32.8	33.5
F4	73.1	33.1	32.1	34.8
F5	57.7	21.2	27.2	21.9
F6	44.2	14.7	17.5	14.6

In Table 4.3, the results are taken in the analyses at the 2.0% roof drift ratio. At this point, some of the columns started to yield and wall started to increase its load carrying capacity. In all loading cases, the inelastic base shear force ratio of wall is significantly below the elastic base shear force ratio of wall.

4.3 NONLINEAR DYNAMIC ANALYSES

In this section, the behavior of the buildings under eight different earthquakes records whose details were given in Section 3.5 will be discussed. The earthquakes records are scaled to the proposed earthquake spectra by TEC. Total masses are lumped in the corresponding nodes. Due to the scaling of the earthquake records, the responses of the structures are expected to be similar to each other.

4.3.1 Time-History Analyses Results

Maximum roof drift and inter-story drift ratio of building are investigated through Figure 4.22 to Figure 4.30. The purpose herein is to investigate analytically the general response of a reinforced concrete frame-wall structure under eight different scaled earthquakes records.

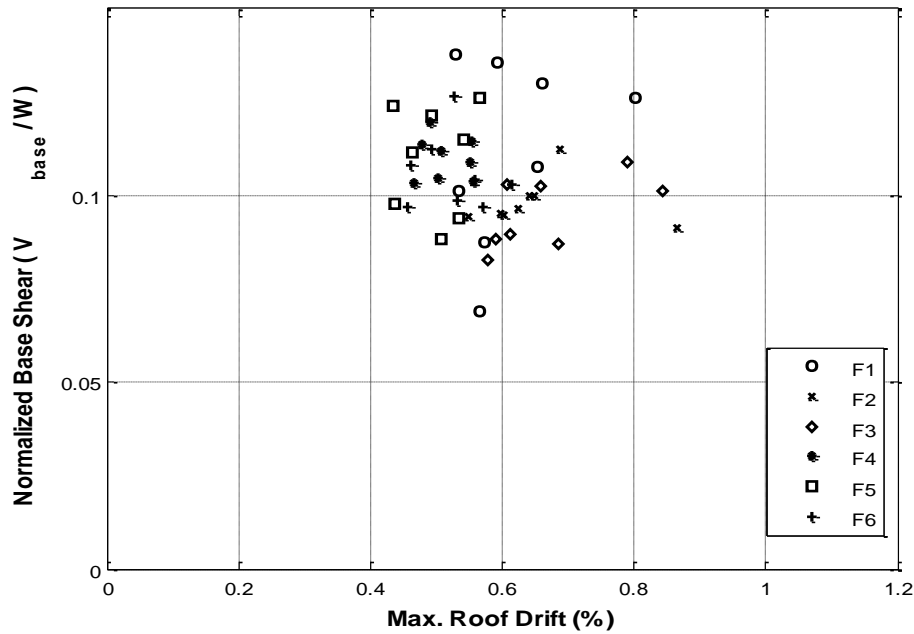


Figure 4.22 Normalized Base Shear vs. Maximum Roof Drift for All Buildings – Time-History Analysis

In Figure 4.22, the absolute maximum roof drift of six buildings under eight scaled ground motions is plotted against the absolute maximum of the normalized base shear. The absolute maximum roof drift and normalized base shear is plotted at same time. From this figure, it is understood that the buildings are in the plastic range since the wall is known to yield at 0.5% roof drift from prior analyses. The maximum roof drift ratio is 0.83% in Figure 4.22, which means the buildings should survive under the scaled earthquakes during time-history analyses. In the next figures, the inter-story drift ratio of the buildings is presented.

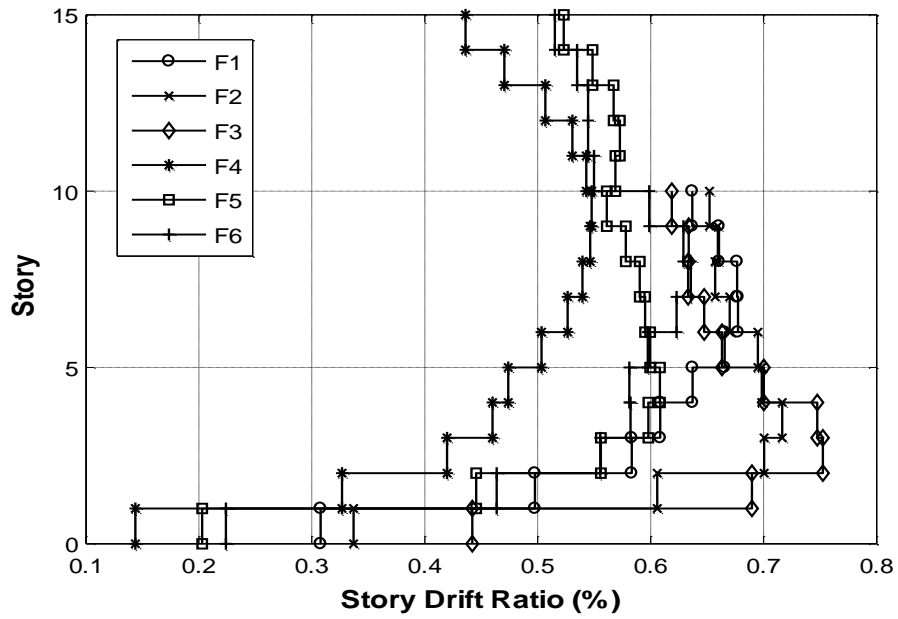


Figure 4.23 Story vs. Max. Inter-Story Drift Ratio for All Buildings – Time-History Analysis of Gm1

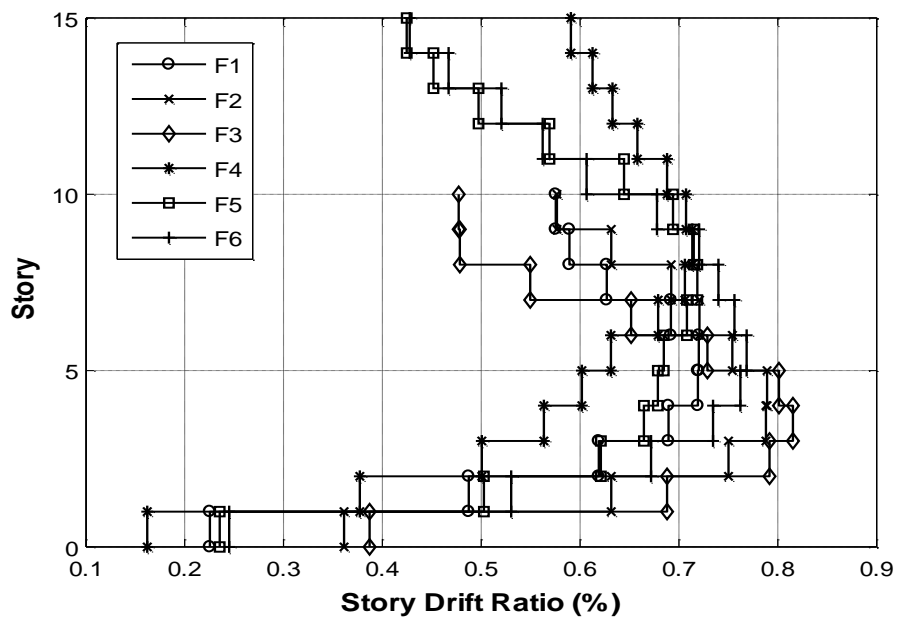


Figure 4.24 Story vs. Max. Inter-Story Drift Ratio for All Buildings – Time-History Analysis of Gm2

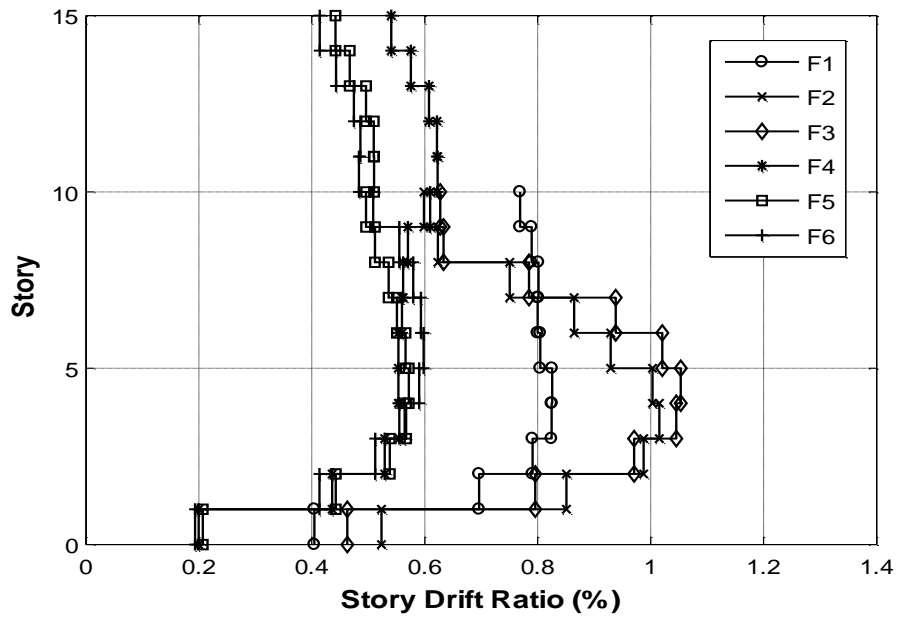


Figure 4.25 Story vs. Max. Inter-Story Drift Ratio for All Buildings – Time-History Analysis of Gm3

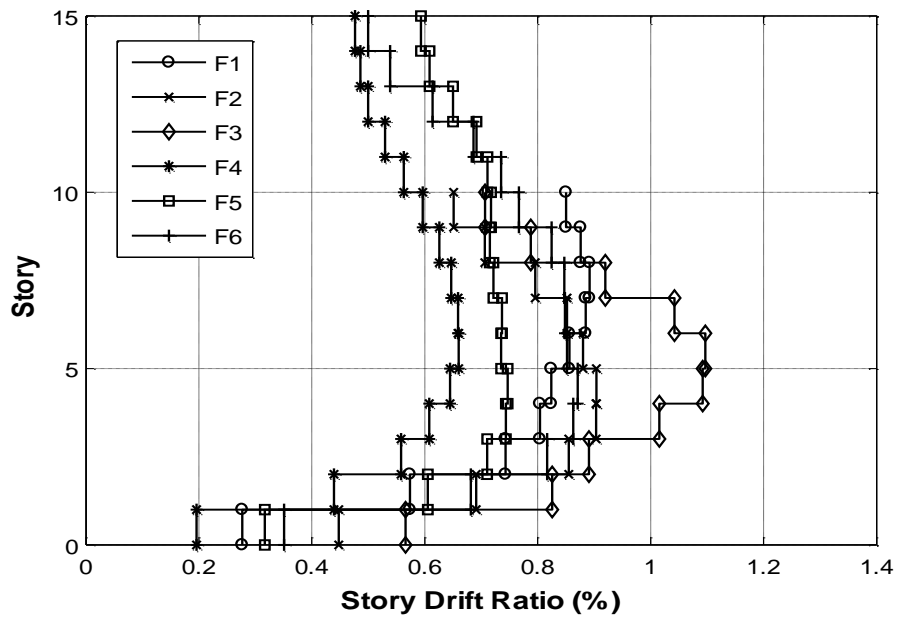


Figure 4.26 Story vs. Max. Inter-Story Drift Ratio for All Buildings – Time-History Analysis of Gm4

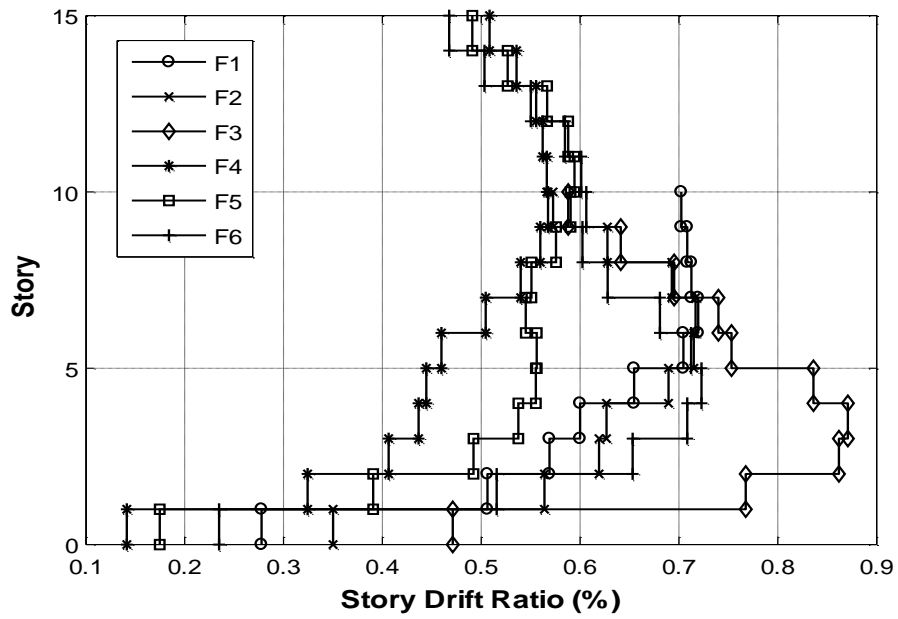


Figure 4.27 Story vs. Max. Inter-Story Drift Ratio for All Buildings – Time-History Analysis of Gm5

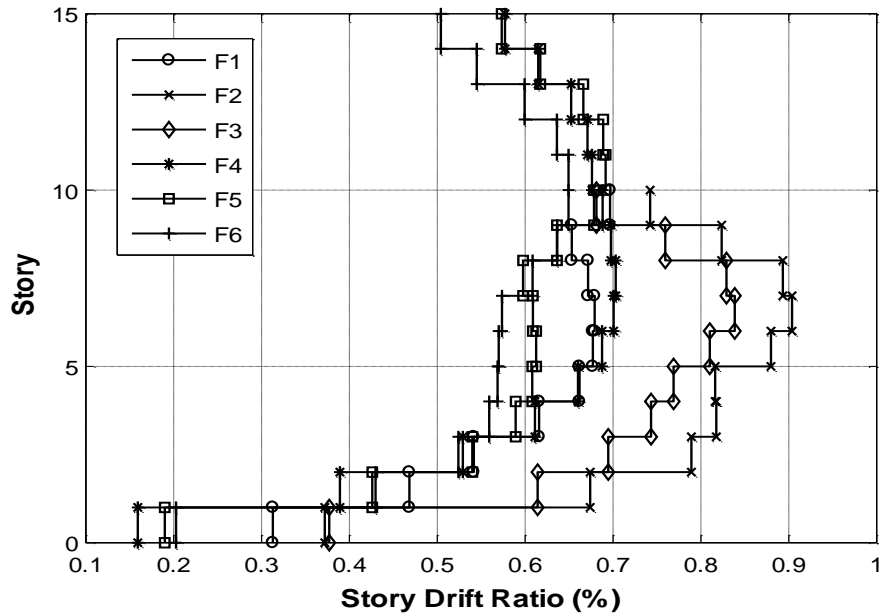


Figure 4.28 Story vs. Max. Inter-Story Drift Ratio for All Buildings – Time-History Analysis of Gm6

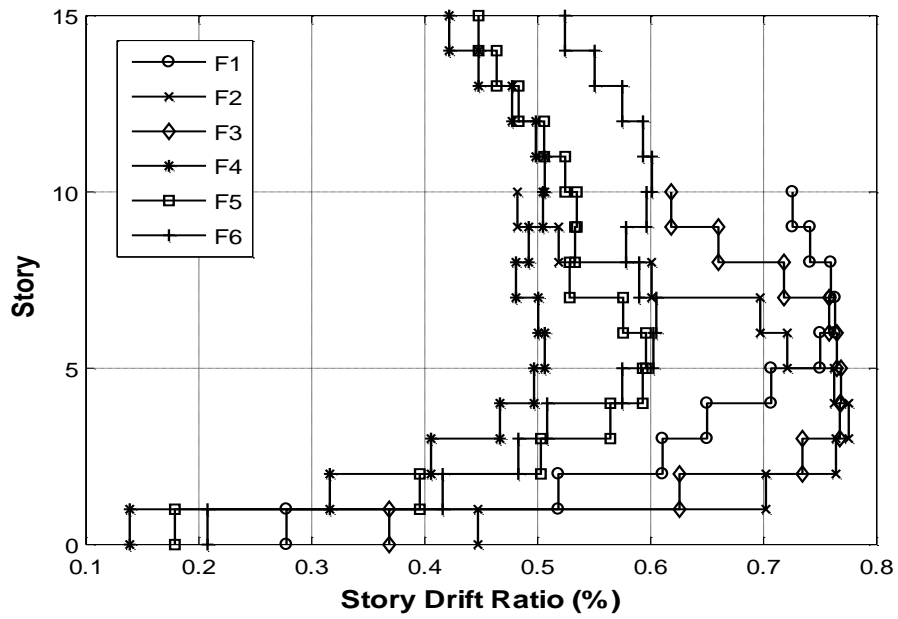


Figure 4.29 Story vs. Max. Inter-Story Drift Ratio for All Buildings – Time-History Analysis of Gm7

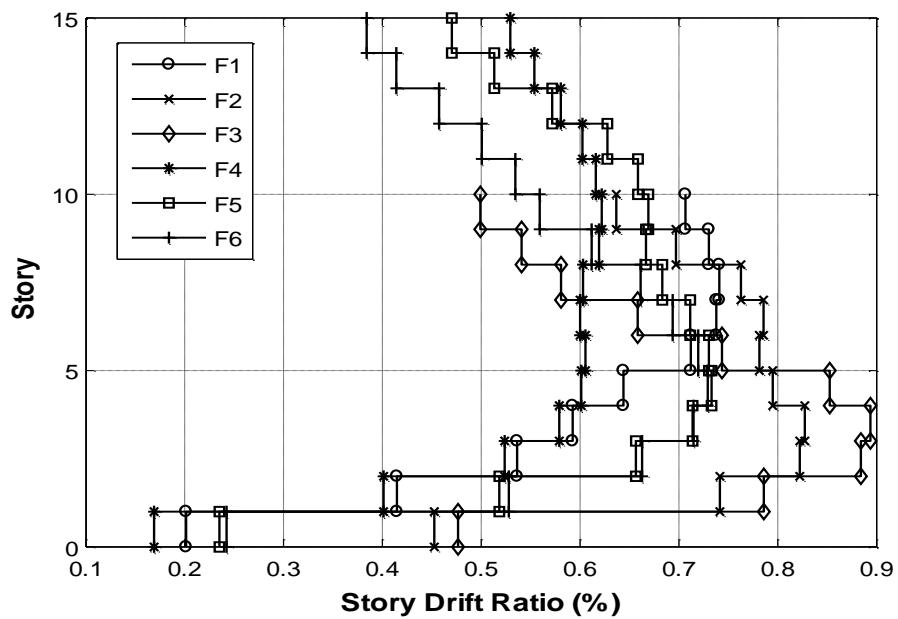


Figure 4.30 Story vs. Max. Inter-Story Drift Ratio for All Buildings – Time-History Analysis of Gm8

Through Figure 4.23 to 4.30, maximum envelopes of inter-story drift ratio of all buildings are shown. Some of the time-history analyses yield similar results. Gm4, Gm5 and Gm8 produce similar results for inter-story drift. F3 has the strongest lateral load strength, but in the time-history analyses for Gm1 and Gm3 it produces the largest inter-story drift ratio at fourth story. It is clear that rapid change in maximum inter-story drift ratio is observed at the second story of the buildings. Moreover, the time-history analyses results do not depend on the base shear ratio of wall and building height.

Despite the fact that the ground motions were scaled with respect to the design response spectrum proposed by TEC, differences in inter-story drifts were observed as a result of the nonlinear dynamic analysis of the buildings. It is important to realize that the scaling procedure obviously does not produce exactly the same type of ground motion despite the behavior observed in the spectral acceleration shown in Figure 3.12. Differences are for example due to the duration of the ground motions, the time where the peak accelerations occur for the scaled ground motions. Further differences will be discussed in local responses measures in the next.

4.3.2 Plastic Rotation of Selected Elements

In this section, maximum plastic rotations of wall and middle column (See Figure 3.1) are discussed under different scaled ground motions for detailed investigation of the local response measures of the buildings.

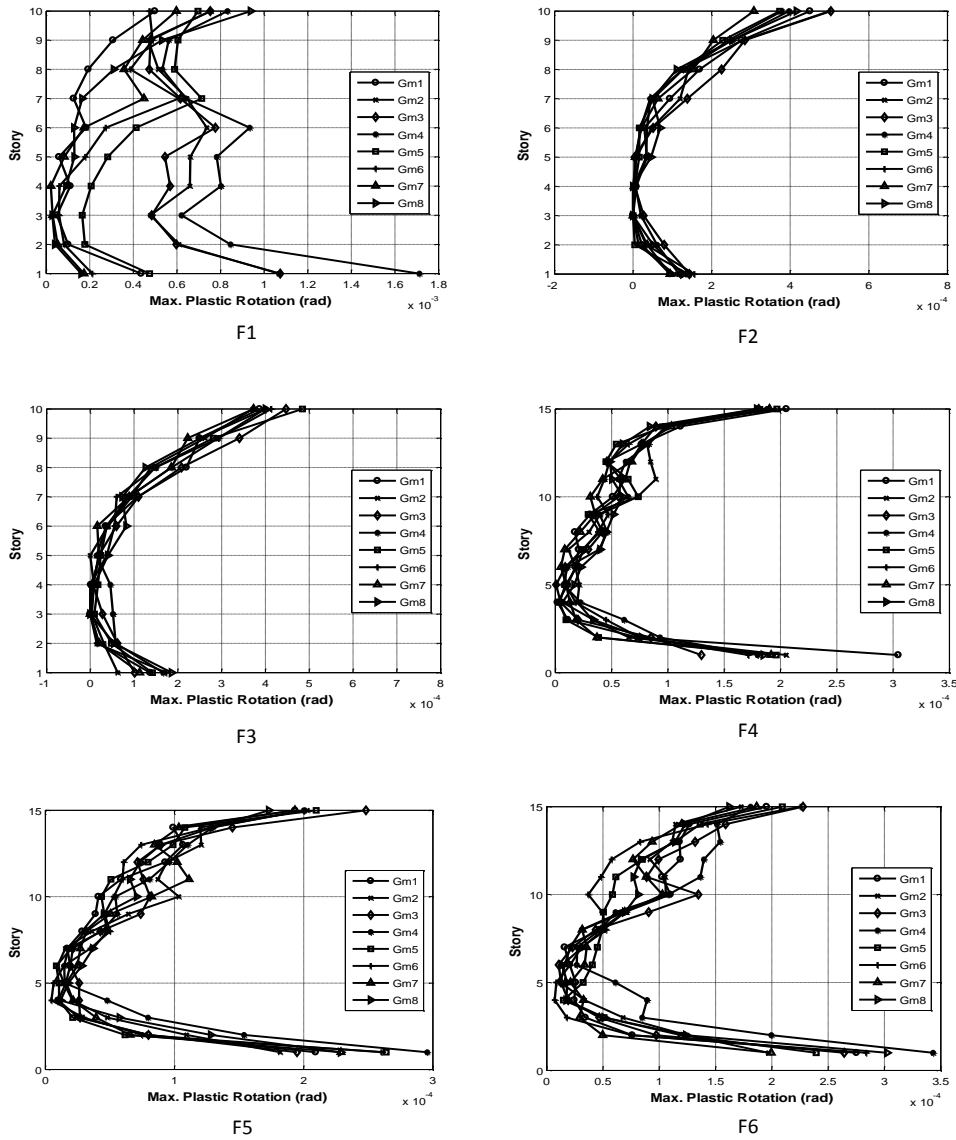


Figure 4.31 Plastic Rotation of Middle Column – Time-History Analysis

In Figure 4.31, maximum envelopes of plastic rotations of the middle column (See Figure 3.1) of the buildings are given. In Figure 4.31, at second story, the concentration in plastic rotation is seen for all buildings. 15-story buildings have more plastic rotation at base level than 10-story buildings. It is interesting to observe that the base shear force ratio of wall does not affect the plastic rotations. Except F1, ground motions produces similar results. The difference in F1 may

depend on the property of F1 because F1 has lowest lateral load strength and the plastic rotations of F1 is almost 10 times bigger that other buildings.

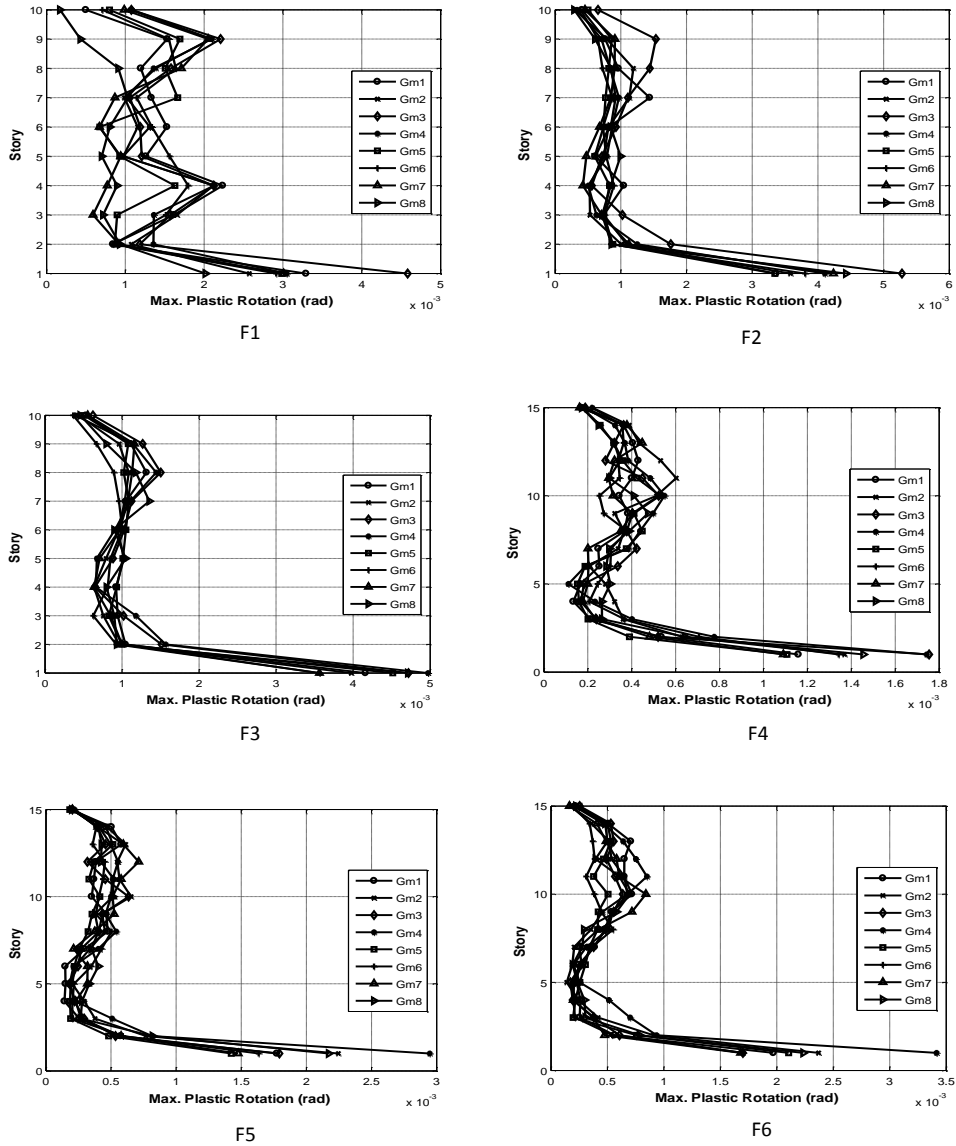


Figure 4.32 Plastic Rotation of Wall – Time-History Analysis

In Figure 4.32, maximum envelopes of plastic rotations of wall of the buildings are given. At second story, the concentration in plastic rotation in wall is seen in

all buildings. For 10-story buildings, the plastic rotation does not depend on the building and 10-story buildings produce similar results. For 15-story buildings, the plastic rotation do not depend on the building and 15-story buildings produce similar results. The plastic rotations in the wall do not depend on the height of the building but F1 produces different plastic rotation patterns. This result might be caused due to the interaction between wall and frame because the middle columns produce non-stable plastic rotations for F1 building. It can be concluded that the wall of F4 building is exposed to least plastic rotation because F4 has great lateral strength and high base shear force ratio of wall.

4.3.3 Patterns of Shear Force Distributions

In this section, absolute maximum envelopes of shear force distributing along stories of columns and wall for dynamic analyses are presented in Figure 4.33 and Figure 4.34. It is important to understand the shear force distribution along stories because they give meaningful results for understanding the inelastic force distribution between wall and frame. To understand these, nonlinear dynamic shear force distribution along stories are discussed in this section.

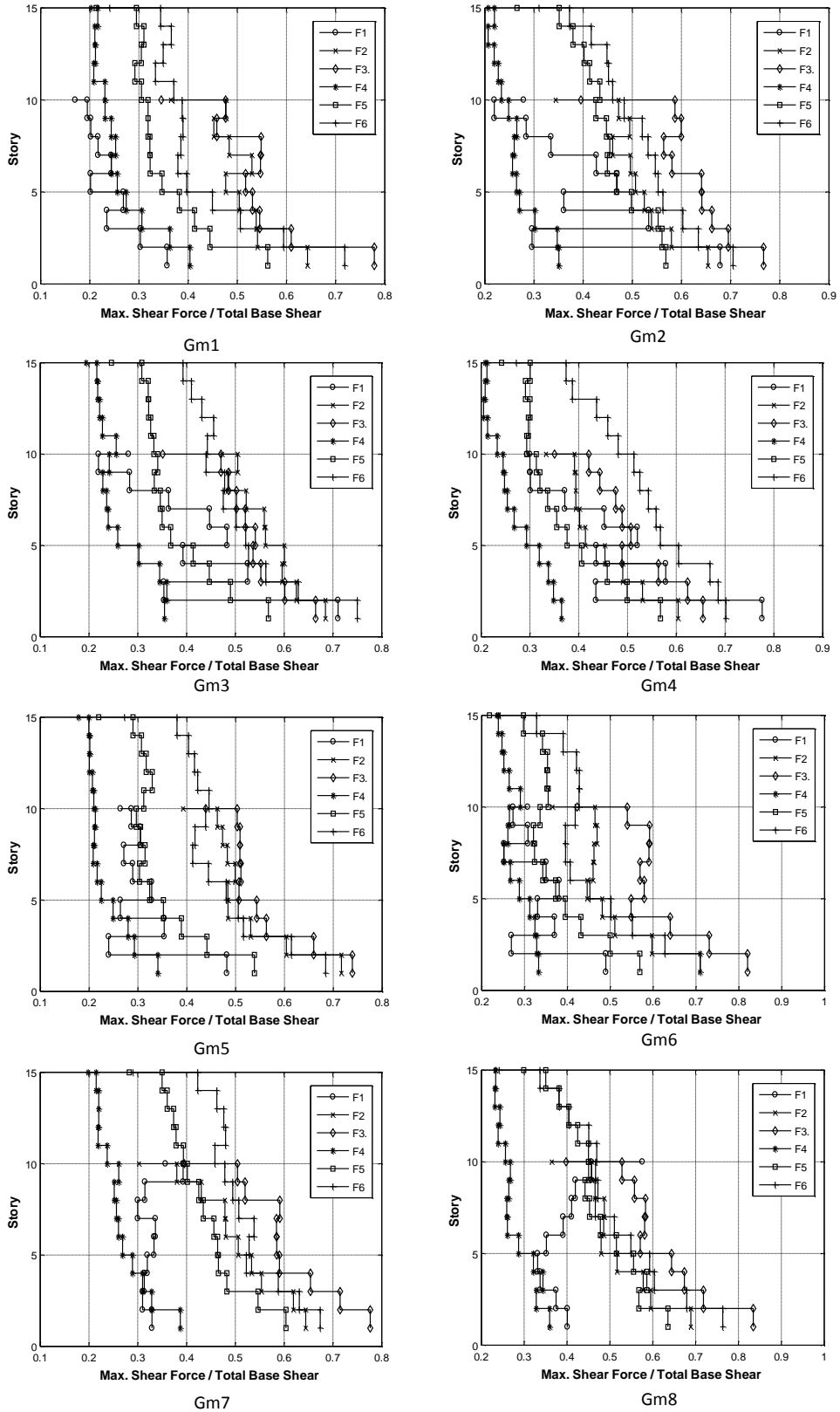


Figure 4.33 Story vs. Maximum Total Shear Force / Total Base Shear for Columns – Time-History Analysis

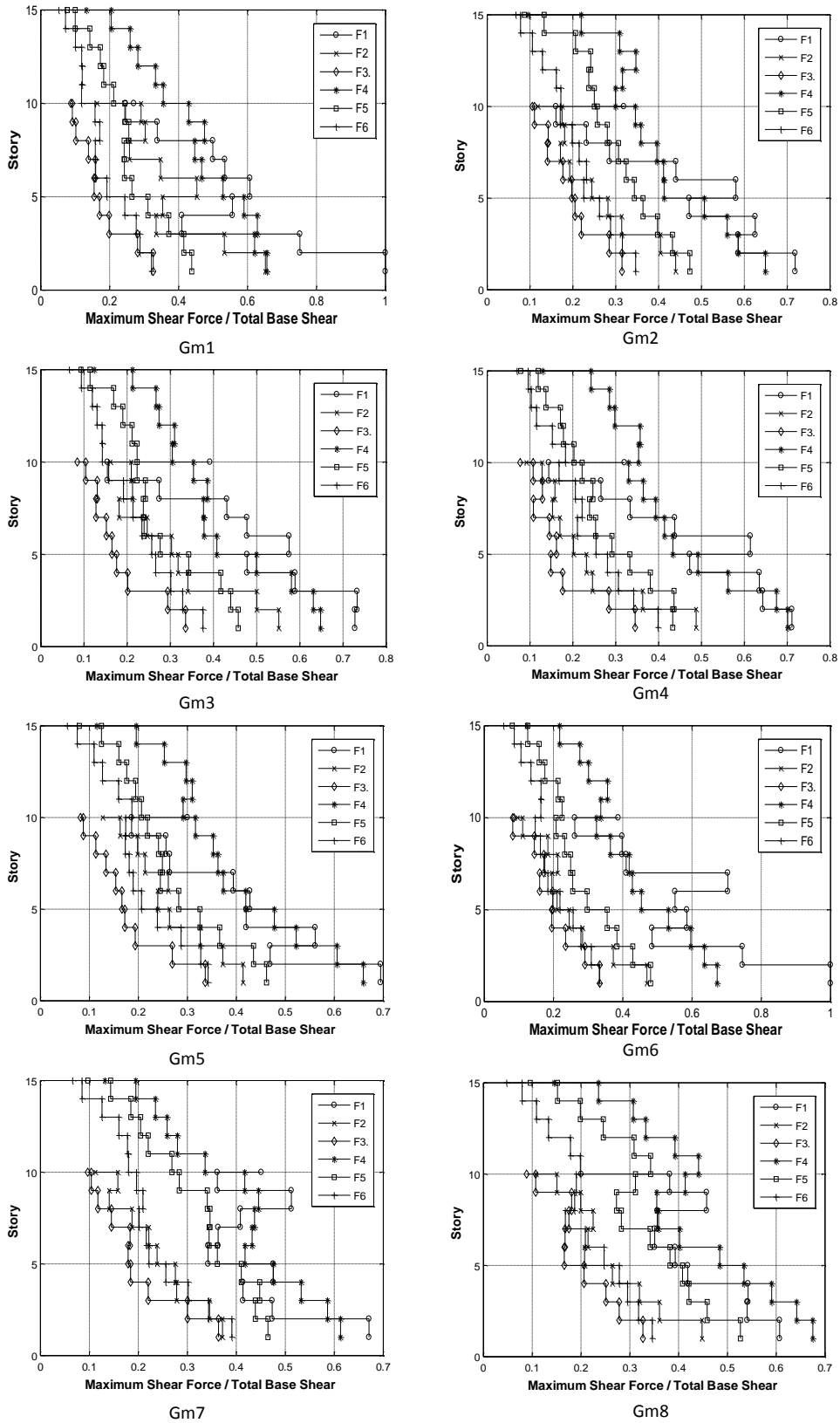


Figure 4.34 Story vs. Maximum Shear Force / Total Base Shear for Wall – Time-History Analysis

In Figure 4.33, the absolute maximum shear force of the columns is shown. In this figure, eight ground motions are used and the details of the ground motions were given in Section 3.5. The shear force ratio changes from 34 % to 83 %. It means that the base shear force ratio is different from the time-history and elastic analysis. Moreover, the observation from the maximum shear force envelope can be misleading since the maximum force envelopes do not occur at the same time. This phenomenon can yield wrong results such that the summation of shear force percentage can be over hundred percentages. In addition, due to the hysteretic properties of the material model, the maximum shear force can be misleading for comparing time-history analyses of two different ground motions because the reloading numbers of building are not known well for different analyses.

In Figure 4.33, the shear force distribution of columns increases along stories as the base shear ratio of wall decreases. However F2 and F3 produce similar distribution in some ground motion analyses. Analysis of F1 under Gm2 ground motion results in interesting shear force distribution. This situation may be observed because of the local failures of columns. Moreover, F1 building is the weakest building and this affects the result.

In Figure 4.34, the absolute maximum shear force of the wall is shown. It is understood that the shear force ratio changes from 30% to 100%. Thus, in some cases, the shear wall can take all of the shear force, because local failure of the columns can result in no shear force in that element. The maximum envelopes of shear force of wall can be misleading due to the same reason explained above for columns.

4.4 SUMMARY

In this chapter, six buildings were investigated under pushover analysis and time-history analysis. For pushover analysis, three lateral load patterns were used as triangular, uniform and first-mode lateral load pattern. The pushover analyses were done by using OpenSEES. In the analysis stage, some problems were encountered. First of all, convergence problems were encountered during the solution of the nonlinear equilibrium equations with the nonlinear algorithms available in OpenSEES. It is observed that the Krylow Newton (Mazzoni et al., 2007) algorithm solved most of these problems in this regards. Another problem was observed due to the use of rigid links in connecting the nonlinear frame elements having fiber sections. In order to overcome this problem one axially rigid element was used at each story level. Moreover, besides the buildings in Chapter 3, three more buildings were designed and modeled in the preliminary stage of the research conducted in this thesis. The pushover responses of these buildings had stability and convergence problems close to 2% roof drift ratio; thus these were not considered as sufficiently ductile for parametric analyses conducted in this thesis. The encountered problems were caused by the level of axial force in the load carrying components. To fix this problem the width and thickness of wall was multiplied by 1.5 and the new buildings were designed.

For static pushover analysis, triangular and first-mode lateral load patterns produced similar results and uniform lateral load pattern produced more lateral load under same top story drift ratio, thus the members cracked earlier under uniform loading. The nonlinear behavior of the wall did not change under different building height, because the width of wall was 3 m and same top story drift ratios produced same total rotation in the wall, therefore, the strain at the edge of wall is same for all buildings and the edge steel of wall yields at same top story drift ratio for same material model. The nonlinear properties of the column were different, because the section properties changes for all buildings. Moreover,

the force redistribution between wall and columns were worth to be investigated, because similar pushover results were produced for all buildings. The wall yielded at 0.5% top story drift ratio, but the necessary strength for stable drift ratio was supplied by columns. After columns started to crack, the required strength was supplied by wall because the wall performed perfect ductile performance by itself and it had necessary strength for ductile performance. Therefore, it could supply the required strength for ductile response. For wall, the plastic rotation for the buildings, which had same base shear force ratio under different building height, was similar because the wall width was same and the wall width dominates the nonlinear behavior of the wall. However, the columns produced different results for the buildings, which had same base shear force ratio under different building height, because the section properties of columns changed for those buildings.

Afterwards, time-history analysis was carried out by using OpenSEES. Convergence problems encountered were overcome by decreasing the time increment and by utilizing Newton Line Search (Mazzoni et al., 2007) algorithm. It is worth to mention that decreasing the step actually resulted in increased amount of data to be stored for post processing.

For time-history analysis, eight scaled ground motions, whose details were given in Section 3.5, were utilized. The scaling was made using Rspmatch (Fahjan and Ozdemir, 2008). The absolute maximum roof drift ratio was 0.83% and minimum roof drift ratio was 0.42%. Therefore, yielding occurred in the walls and columns. Maximum plastic rotations were similar for the wall for different height, but maximum plastic rotations were different for columns, because the dimensions of the wall was same for different height and column dimensions were different for different height.

CHAPTER 5

CONCLUSION

5.1 CONCLUSION

The modeling of the inelastic behavior of reinforced concrete structures is a complicated problem, but by adopting simple assumptions and analytical procedures described in this thesis, reasonable results are obtained. Using realistic constitutive models for concrete and steel materials, and advanced finite element models to capture spread of plasticity in structural members, leads to extra computational effort, but remarkable improvements can be achieved. Considering these results, the following statements are achieved from this study:

- Initial base shear percentages of wall in nonlinear lateral load analyses are significantly higher than those in elastic analyses.
- Load redistribution occurs between wall and frame parts due to the yielding of wall at 0.5% roof drift ratio. The softening in wall does not change the general smooth drift behavior of building because the columns supply the required strength necessary to ensure ductile yielding of the building. Once the base columns yield at around 1.8% roof drift in this study, it is observed that the walls then again supply the required strength to the structural system. Thus, it is observed that the ductility of wall members in wall-frame systems is the most crucial element in ensuring the

overall ductile response of these buildings no matter what the wall percentage is with respect to the frame.

- Due to the overturning effect, lateral load carrying capacity of exterior columns reduces significantly due to the excessive axial loads. However, it is observed that the axial load carrying capacity remains in these members, and the overturning effect does not significantly alter the overall behavior of the structure.
- Rapid change in inter-story drift ratio is observed in frame parts of the buildings despite the fact that the design is fully compatible with TEC (Turkish Earthquake Code 2007) and Turkish Standards TS500, and furthermore checked with regards to the finite element package Probina. Despite the fluctuations in inter-story drift ratio, wall provides the required strength for stability of building.
- The behavior of frame-wall buildings resembles each other, because the width of wall dominates the nonlinear behavior of wall and the wall usually controls the nonlinear behavior of the building.
- Plastic rotations of wall show that the wall is a good energy dissipating member of the buildings.
- In pushover analyses, triangular and first-mode lateral load pattern produce similar results in the buildings, and uniform lateral load pattern punishes the building more than the other loading cases.
- Time-history analyses with scaled ground motions produces similar roof drift ratio of a building in terms of general response of a building, but it produces completely different inter-story drifts and member forces in

terms of local response measures of a building. Thus, these differences would require further attention in the design phase.

5.2 RECOMMENDATIONS FOR FUTURE RESEARCH

The following considerations are recommended for future research:

- For mid-rise reinforced concrete buildings, different width of walls should be compared in the nonlinear analyses.
- Concentration of inter-story drifts in columns of frame-wall structural systems should be carefully followed for the building designed in the limits of the TEC.

REFERENCES

Akiş, T. (2006), *Lateral Load Analysis of Shear Wall–Frame Structures*, Ph.D. Thesis, Middle East Technical University, Ankara.

Amiri, J., Ahmadi, Q., Ganjavi, B. (2008), *Assesment of Reinforced Concrete Buildings with Shear Wall Based on Iranian Seismic Code*, *Journal of Applied Sciences*, Vol. 8, No. 23,

Clark, W., J. (1968), *Analysis of Reinforced Concrete Shear Wall-Frame Structure*, Ph.D. Thesis, University of Alberta, Ottawa, Canada.

Emori, K., Schnobrich, W. (1978), *Analysis of Reinforced Concrete Frame-Wall Structures for Strong Motion Earthquakes*, Report No. UILU-ENG 78-2025, National Science Foundation, University of Illinois, Illinois, USA.

Fahjan, Y., Ozdemir, Z. (2008), *Scaling of Earthquake Accelerograms for Non-Linear Dynamic Analyses to Match the Earthquake Design Spectra*, *the 14th Word Conference on Earthuake Engineering*, Beijing, China.

Goodsir, W., Paulay, T., Carr, A. (1982), *The Inelastic Seismic Response of Reinforced Concrete Frame-Shear-Wall Structures*, Research Report, University of Canterbury, Christchurch, New Zealand.

Karsan, I., D., Jirsa, J., O. (1969), *Behavior of Concrete under Compressive Loadings*, *Journal of the Structural Division*, American Society of Civil Engineers, New York, Vol. 95, 2543-2563.

Kayal, S. (1986), *Nonlinear Interaction of RC Frame-Wall Structures*, *Journal of Structural Engineering*, Vol. 112, No. 5.

Kent, D., C., Park, R. (1971), Flexural Members with Confined Concrete, *Journal of the Structural Division*, American Society of Civil Engineers, New York, Vol. 97, ST7.

Mazzoni, S., McKenna, F., Scott, M., and Fenves, G. (2009). *OpenSEES Command-Language Manual*. Retrieved from <http://opensees.berkeley.edu>, 27/07/2011.

Orakcal, K., Wallace, J., W. (2006), Flexural Modelling of Reinforced Concrete Walls – Experimental Verification, *ACI Structural Journal*, Vol. 103, No. 2, page 196-206

Pacific Earthquake Engineering Research Center (PEER), *Strong Motion Database*, Retrieved from <http://peer.berkeley.edu/> 21/04/2011.

Probina (2010), Probina for Microsoft Windows, version 15.0 (2010). *Reference Guide Manual*. Ankara: Prota Bilgisayar.

Reyes, J., Chopra, A. (2011), Modal Pushover-Based Scaling of Two Components of Ground Motion Records for Nonlinear RHA of Buildings, Retrieved from <http://nsmpr.wr.usgs.gov/> 25/07/2011.

Schnobrich, W. (1977), Behavior of Reinforced Concrete Structures Predicted by the Finite Element Method, *An International Journal*, Computers and Structures, Vol. 7, No. 3 page.

Takayagani, T., Schnobrich, W. (1976), *Computed Behavior of Reinforced Concrete Coupled Shear Walls*, Report No. UILU-ENG-76-2024, National Science Foundation, University of Illinois, Illinois, USA.

Taucer, F., F., Spacone, E., and Filippou, F., C. (1991), *A Fiber Beam-Column Element for Seismic Response Analysis of Reinforced Concrete Structures*, Report No. UCB/EERC-91/17, California Department of Transportation, National Science Foundation, Earthquake Engineering Research Center, College of Engineering, University of California, Berkeley.

Tjhin, T., Aschheim, M., Wallace, J. (2007), Yield Displacement-based seismic design of RC wall Buildings, *Engineering Structures*, Vol. 29, page 2946–2959.

TS 498 (1987), *Design Loads for Buildings*, Turkish Standards Institution, Ankara.

TS 500 (2000), *Requirements for Design and Construction of Reinforced Concrete Structures*, Turkish Standards Institution, Ankara.

Turkish Earthquake Code, TEC, (2007), *Specification of Buildings to be Built in Disaster Areas*, The Ministry of Public Works and Settlement, Ankara.

Wilson, E., L., Dovey, H., H., Habibullah, A. (1997), “ETABS Three Dimensional Analysis of Building Systems”, *Computers and Structures Inc.*, Berkeley, California, USA.